University of Washington
Department of Civil and Environmental Engineering

EVALUATION OF DATA REQUIREMENTS FOR GROUNDWATER CONTAMINANT TRANSPORT MODELING

Eric W. Strecker
Wen-Sen Chu
Dennis P. Lettenmaier

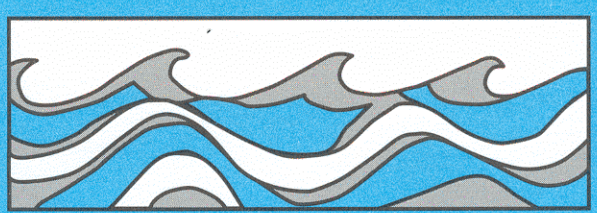

Water Resources Series
Technical Report No.94
May 1985

Seattle, Washington
98195

Department of Civil Engineering
University of Washington
Seattle, Washington 98195

EVALUATION OF DATA REQUIREMENTS FOR GROUNDWATER CONTAMINANT TRANSPORT MODELING

Eric W. Strecker
Wen-Sen Chu
Dennis P. Lettenmaier

Water Resources Series
Technical Report No. 94

May 1985

University of Washington
Department of Civil Engineering
Seattle, Washington 98195

Evaluation of Data Requirements for Groundwater Contaminant Transport Modeling

by

Eric W. Strecker
Wen-sen Chu
Dennis P. Lettenmaier

Water Resources Series
Technical Report No. 94
May 1985

ABSTRACT

Groundwater flow and contaminant transport models have been widely used for planning and design purposes in the past decade. The predictive ability of these models is limited by the assumptions and approximations introduced in the model governing equations and their solutions, the model parameters used, and the availability and quality of the model calibration data. By combining a parameter identification algorithm with the United States Geological Survey's Method of Characteristics (USGS-MOC) Code and using two synthetic aquifers, this study evaluated the effects of data availability and uncertainty on groundwater contaminant transport prediction by a series of numerical experiments. The study results indicate that the predictive ability of USGS-MOC is limited unless relatively extensive and good quality data are available. Extending the time length of observation was generally more effective in improving parameter estimates than adding more observation wells. Finally, provided that all boundary conditions are known, the accurate estimation of transmissivity in an aquifer is by far the most important step toward more reliable prediction of contaminant transport. The experimental results showed that when only limited data were available for model calibration, the predicted contaminant concentrations could be significantly in error in just five years of simulation. Based on the study results, we suggest that with typical data bases, groundwater flow and contaminant transport model results should be accompanied by detailed uncertainty analysis prior to implementation for planning or design purposes.

ACKNOWLEDGEMENTS

The work upon which this publication is based was supported in part by funds provided by the U.S. Department of the Interior, Bureau of Reclamation, Office of Water Research, under Bureau Grant No. 4-FG-93-00010, superseded by Geological Survey Grant No. 14-08-0001-G-1059.

The study was jointly supervised by Co-Investigators Wen-sen Chu and Dennis P. Lettenmaier, Department of Civil Engineering, University of Washington. The computer experiments were designed and conducted by Margaret Michalek and Eric W. Strecker, and the study served as the basis for Mr. Strecker's Master of Science in Engineering thesis.

We would like to thank Lori Nagle and Stephanie Boyd for their help in the typing and editing of this document, and Don Althauser for assistance with the graphics.

DISCLAIMER

TABLE OF CONTENTS

LIST OF FIGURES

LIST OF FIGURES (cont.)

LIST OF FIGURES

LIST OF FIGURES (cont.)

LIST OF TABLES

LIST OF TABLES (cont.)

CHAPTER 1

INTRODUCTION

Numerous computer simulation models have been developed in the last 20 years to aid in the prediction of groundwater and groundwater contaminant movement, and to assist in the management of groundwater resources. These models characterize groundwater flow and transport with varying levels of simplification, and may be either deterministic or stochastic. The predictive ability of the models is limited by the assumptions and approximations introduced in the governing equations and their solutions, the model parameter values used, and the availability and quality of the data for model calibration. For these reasons, different models may yield substantially different results when applied to the same problem, and in fact, the use of the same model by different users may lead to dissimilar results (McLaughlin, 1984). The two principal reasons for these inconsistencies between models and model users are dissimilarities in model structure, and the judgmental aspects of the identification of model parameters. While the status of the model is beyond the control of the user, once the model selection process has been completed, data availability plays a strong role in the calibration process, and the user generally maintains some control over this stage of the model implementation process.

The objective of this study was to evaluate the effects of data availability and uncertainty on groundwater contaminant transport prediction. Insofar as possible, it was desired to conduct the evaluation in a realistic setting that reflected the conditions encountered in field applications. However, due to the complexity of natural aquifers and the absence of extensive field data that could be assumed to be representative of a "typical"

aquifer, the use of field data was precluded. Instead, this study was conducted with a hypothetical aquifer that had geologic and hydrologic characteristics similar to selected real sites. The characteristics of the hypothetical aquifer were defined independently by a hydrogeologist at the beginning of the study. With the exception of some limited point estimates of aquifer parameters at chosen observation sites, the aquifer's characteristics were kept from the investigators until the end of the study.

Using externally defined aquifer characteristics and known boundary conditions, pumping schedules, and contaminant source loading, the aquifer responses were simulated using the United States Geological Survey's Method of Characteristics (USGS-MOC) Code (Konikow and Bredehoeft, 1978). The aquifer responses were taken to be the underlying (true) statistical population and, like the aquifer characteristics, were unknown to the investigators until the end of the study. The USGS-MOC Code was selected as the generating model because it was thought to incorporate the essential detail that would be present in a real aquifer response. From the USGS-MOC generated data, samples of head concentration were taken, which were assumed to represent monitoring data, such as would be available for model calibration in a real application. The model parameters were calibrated based on these samples, and model predictions using the estimated parameters were compared with the true heads and concentrations. To provide a realistic representation of actual field data, a spatially and serially correlated perturbation field was added to the deterministic model realizations to represent realistic field samples. The magnitude of the perturbations and their correlation structure was varied to reflect a range of variabilities associated with model predictions of head and concentration and the errors found in the sampling.

To assess the effects of data availability and quality on parameter estimates and therefore model predictive accuracy, six sampling strategies were investigated. Each strategy was defined by the length of record, and number and spatial distribution of observation wells. Each of the sampling strategies was evaluated with three levels of additive uncertainty in heads and concentrations, and several assumed spatial variation patterns for transmissivity.

Given the large number of cases to be evaluated, it was essential to automate the parameter estimation procedure. This was accomplished using a quadratic programming optimization method originally introduced to parameter identification problems by Yeh (1975). Automation of the parameter estimation process had the additional advantage that it eliminated most of the variability in parameter estimates that would otherwise have been associated with subjective factors. The parameter identification (PI) method was formulated as an ordinary constrained least squares problem which minimizes the discrepancies between model solutions and observations.

The next chapter of this report presents a literature review of some recent groundwater contaminant transport studies and a review of calibration methods with particular emphasis on data requirements and model predictive uncertainty. Chapter 3 describes the USGS-MOC model and the assumptions made by the model, while Chapter 4 describes the proposed PI algorithm and the numerical examples used to test the code combining the PI algorithm and USGS-MOC model. Chapter 5 describes the random field noise generator that was created for this study. Chapter 6 outlines the experimental procedure, including a description of the synthetic aquifer, the chosen sampling strategies, parameterization of transmissivities, and the noise levels superimposed on the synthetic observations. The numerical results from the

experiments are given and discussed in Chapter 7. The conclusions are presented in Chapter 8.

CHAPTER 2

LITERATURE REVIEW

Many mathematical models of groundwater flow and solute transport have been developed in the past twenty years (e.g. Remson et al., 1971; Bachmat et al., 1980; Pinder and Gray, 1977; Wang and Anderson, 1982; and Javandel et al., 1984). These models have been formulated to examine a variety of aquifer properties and conditions. Numerical solution methods used include finite differences (Remson et al., 1971), finite elements (Pinder and Gray, 1977), the boundary integral method (Ligget and Liu, 1982), the integrated finite difference technique (Narasimhan and Witherspoon, 1976), and the method of characteristics (Reddell and Sunada, 1970), and random walk scheme (Prickett et al., 1981).

All of these models contain some site-specific parameters that must be calibrated with available observations of the aquifer. There are two approaches to model calibration. The first approach is a trial and error process, in which selected parameter values are varied until the match between model predictions and observations are judged satisfactory. Numerous modeling studies were reviewed; almost all used conventional trial and error methods for model calibration. A few recent examples of particular interest to contaminant transport modeling are reviewed below.

Cohen and Mercer (1984) used the two-dimensional, cross-sectional model, SATUNA (Neuman, Feddes, and Bresler, 1974) to model flow through a typical geological cross-section between Love Canal and Caysga Creek in New York. The model was calibrated for steady-state and transient conditions. Predictive simulations for 50 years were performed to evaluate the changes in the flow field of a proposed synthetic cover and concrete cutoff wall. Qualitative

remarks were made about the effect on contaminant migration of changes in the flow field.

Buller, Gradet, and Reed (1984) used the Illinois Random Walk Solute Transport Model (TRANS) (Prickett et al., 1981) to help define the potential plume geometry and determine the maximum well spacing for a proposed hazardous waste facility located in the upper Gulf of Texas. Skaggs (1984) also used the TRANS model to assess selected mitigation strategies to control radionuclide migration in an aquifer located in the Gulf Coast plain of Texas. Using limited data, a regional steady-state flow model was calibrated first. Trial and error adjustments of hydraulic conductivity and recharge were made to match model solutions with observations. Using the boundary conditions determined from the regional flow model and assumed longitudinal and transverse dispersivities, TRANS was used to determine the effects of different mitigation strategies on contaminant migration over a 1000-year horizon.

Wang and Williams (1984), in a study of seepage from a uranium mill slurry pond in Wyoming, found that field data are seldom, if ever, adequate to define a unique solution from a mathematical model. Yakowitz and Duckstein (1980) reached a similar conclusion from a theoretical analysis. Wang and Williams contended that an extensive monitoring program would be required to check the effectiveness of the proposed mitigation strategy, which had been based on modeling results. They attempted to calibrate Prickett and Lonnquist's (1971) transient groundwater flow model with a limited number of steady-state well observations and a few pump test estimates.

The trial and error calibration procedure used in the above studies is easy to implement. The actual process however, can be time-consuming and frustrating. Further, trial and error calibration results will vary from user

to user depending on the subjective choices of parameters and the fitting criteria used. An alternative to trial and error calibration is the use of search algorithms to identify those parameters that optimize some function of the fitted and observed state variables (e.g., head and concentrations). This approach, also known as parameter identification (PI), is an automated procedure which searches for model parameters that minimize a function of the discrepancies between model predictions and observations. The most commonly used function is the sum of squares, which has a number of advantages including compatibility with certain specialized optimization algorithms such as quadratic progamming.

The idea of PI has been used in many scientific disciplines for more than twenty years (Bard, 1974). Some of the more recent PI work in groundwater modeling has been reported by Neuman (1973); Frind and Pinder (1973); Yeh (1975); Cooley (1977); Umari, Willis, Liu (1979); Yeh and Yoon (1981); Kitanidis and Vomvoris (1983); Sadeghipour and Yeh (1984); and Yeh (1985). Although the effectiveness of the PI methods is also limited by the available data, the approach is more efficient and objective than trial and error. Most of the above PI applications deal only with groundwater flow modeling.

Sophocleous (1984) used the USGS-MOC model to study salt water contamination from oil field salt brine on the Equus Beds aquifer in Kansas. In the study, a PI method proposed by Cooley (1977) was used to calibrate transmissivities, recharge, and leakage for the model. Data from 78 observation wells were used to calibrate the flow model under steady-state conditions. Parameters were assumed to be constant over two transmissivity zones and two recharge zones. Leakage was assumed constant over the entire aquifer. For the contaminant transport part of the modeling effort, dispersivities were calibrated by trial and error to match observed 1980

concentrations in the aquifer. Predictions to the year 2000 were subsequently made to evaluate the potential threat to water supply wells. Sensitivity analysis of the dispersivities, porosity, and pollutant seepage rates were performed. The parameters found by the PI method produced significantly better estimates of the velocity field than those found by the trial and error method. Sophocleous (1984) also suggested application of the proposed PI approach to field monitoring program design.

In each of the studies reviewed above, the model predictions were found to be significantly affected by the quantity and space-time distribution of the available data, the uncertainty in the data, and the simplifying assumptions made in any model formulation. While improved model calibration techniques, such as PI, can assure that the best use is made of the available data, they are not a substitute for field data.

Gates and Kisiel (1974) considered the value of additional data in calibration of a transient simulation of hydraulic heads in the Tucson basin in Arizona by means of sensitivity analysis. They found the most useful data for improving the model predictions were discharge and recharge information, and transmissivities from pump tests. Having more data on initial water table levels and storage coefficients was less helpful. Gates and Kisiel also noted that the transmissivity values obtained from pump tests at the same well varied greatly, suggesting considerable error in local transmissivity estimates.

McLaughlin (1984) compared three different modeling efforts to assess the effects of increased pumping on the San Andres-Glorieta aquifer in northwestern New Mexico. McLaughlin's study emphasized the predictive uncertainty resulting from judgmental decisions made by each of the modelers in applying the same groundwater flow model. The model used was the USGS two-dimensional

finite difference model by Trescott et al. (1976). The modelers' choice of boundary conditions, discretization of the aquifer, and the calibration effort caused a great disparity in the results, as did the interpretation of transmissivity values from pump tests.

The uncertainties in groundwater and groundwater contaminant predictions are of more than academic interest. In many cases, model predictions form the basis for management decisions that ultimately result in large expenditures. This is particularly true in the area of groundwater contaminant and hazardous waste management. Because of the limited data from which the models were calibrated, the interpretation of such modeling results is subject to error. This study attempts to evaluate the effects of data availability and model uncertainty on the calibrated results of a groundwater contaminant model.

CHAPTER 3

GROUNDWATER FLOW AND CONTAMINANT TRANSPORT MODEL

The groundwater model selected for this study was the United States Geological Survey Method of Characteristics Model (USGS-MOC; Konikow and Bredehoeft, 1978). This model was selected because of its superior solution scheme and its excellent documentation. The model is based on two governing equations describing two-dimensional vertically averaged flow and transport through an aquifer. The flow equation is solved by an alternating direction implicit finite difference method, and the mass transport equation is solved by a combined particle tracking scheme (for convective transport) and a finite difference procedure (for hydrodynamic dispersion). The governing equations and the numerical solution techniques used by USGS-MOC are briefly introduced here.

The equation describing two-dimensional vertically averaged transient flow of a homogeneous incompressible fluid through a nonhomogeneous anisotropic confined aquifer can be written as (Konikow and Bredehoeft, 1978):

$$\frac{\partial}{\partial X_i}\left(T_{ij}\frac{\partial h}{\partial X_j}\right) = S\frac{\partial h}{\partial t} + W \qquad i,j = 1,2 \qquad (3.1)$$

Where

T_{ij} = transmissivity (L^2/t)

h = hydraulic head (L)

S = storage coefficient

t = time

$W = W(X_1, X_2)$ = source/sink term (L/t)

X_i, X_j = two-dimensional Cartesian coordinates (L)

The source/sink term, W, which contains direct withdrawal or recharge, or steady leakage may be described as:

$$W(X_1, X_2) = Q(X_1, X_2) - \frac{K_z}{m}(H_s - h) \tag{3.2}$$

Where

Q = is the rate of recharge or withdrawal (L/t)

K_z = vertical hydraulic conductivity (L/t)

m = thickness of the confining layer, stream bed, or lake bed (L)

H_s = hydraulic head in source bed lake or stream (L)

With the solutions of hydraulic head from Eq. (3.1), the velocity of the groundwater flow is evaluated in the model by Darcy's Law as:

$$V_i = \frac{-K_{ij}}{\varepsilon} \frac{\partial h}{\partial X_i} \tag{3.3}$$

Where

V_i = seepage velocity in direction of X_i (L/T)

K_{ij} = the hydraulic conductivity tensor (L/T)

ε = effective porosity of aquifer (dimensionless)

The equation which describes two-dimensional areal transport and dispersion of a conservative tracer can be written as (Konikow and Grove, 1977):

$$\frac{\partial C}{\partial t} = \frac{1}{b}\frac{\partial}{\partial X_i}\left(bD_{ij}\frac{\partial C}{\partial X_j}\right) - V_i\frac{\partial C}{\partial X_i} + \frac{C\left(S\frac{\partial h}{\partial t} + W - \frac{\partial b}{\partial t}\right) - C'W}{\varepsilon b} \qquad (3.4)$$

$$i,j = 1,2$$

Where

C = concentration (M/L^3)

D_{ij} = dispersion coefficient (L^2/T)

b = saturation thickness (L)

C' = source concentration (M/L^3)

The following assumptions have been made in the formulation of the USGS-MOC model (Konikow and Bredehoeft, 1978):

1. Darcy's law is valid and hydraulic-head gradients are the only significant driving mechanisms for fluid flow.

2. The porosity and hydraulic conductivity of the aquifer are constant with time, and porosity is uniform in space.
3. Gradients of fluid density, viscosity, and temperature do not affect the velocity distribution.
4. No chemical reactions occur that affect the concentration of the solute, the fluid properties, or the aquifer properties.
5. Ionic and molecular diffusion are negligible contributors to the total dispersive flux.
6. Vertical variations in head and concentration are negligible.
7. The aquifer is homogeneous and isotropic with respect to the coefficients of longitudinal and transverse dispersivity.

The flow equation (Eq. 3.1) is solved by an alternating direction implicit finite difference method (Pinder and Bredehoeft, 1968; Remson et al., 1971). The transport equation (Eq. 3.4) is solved in two steps. The advection part of the solute transport equation is first solved by a particle tracking scheme in which tracer particles are advected by velocities determined from Eq. (3.3). Hydrodynamic dispersion effect is calculated in the second step, in which the dispersive transport terms are solved by the finite difference method. Because of the particle tracking scheme, the entire solution procedure was called the Method of Characteristics (MOC) by Konikow and Bredehoeft (1978).

CHAPTER 4

PARAMETER IDENTIFICATION METHOD

The formulation of the parameter identification scheme used in this study and its attachment to the USGS-MOC model is described in this chapter.

PI Formulation

Let us assume that there are M observation wells at which the piezometric head (or water table) and solute concentration are taken over N time periods. If we denote the calculated piezometric head and solute concentration at the i'th observation well, in the j'th time period to be h_{ij} and C_{ij}, respectively, then we can introduce two error functions ε_{ij} and η_{ij}

$$\varepsilon_{ij} = h_{ij} - h_{ij}^{*} \qquad \text{for all } i,j \tag{4.1}$$

$$\eta_{ij} = \log C_{ij} - \log C_{ij}^{*} \qquad \text{for all } i,j \tag{4.2}$$

where h_{ij}^{*} and C_{ij}^{*} are the observed head and concentration at the i'th well in the j'th time period. The purpose of taking the logarithm of C in Eq. (4.2) is to ensure that the differences between large concentration values (in the near field) and small concentration values (in the far field) are equally weighted in the calibration process.

If we further assume that the errors between the solutions and observations are due only to the incorrect parameter values used in the model (the effect of this assumption is discussed later), then we can write:

$$\varepsilon_{ij} = \varepsilon_{ij}(\vec{p}) \qquad \text{for all } i,j \tag{4.3}$$

$$\eta_{ij} = \eta_{ij}(\vec{p}) \qquad \text{for all } i,j \tag{4.4}$$

in which the vector $\vec{p}$ is the model parameter to be adjusted. In using the USGS-MOC code, $\vec{p}$ could include, for example, transmissivity, aquifer thickness, dispersivities, and other aquifer parameters.

Expanding Eqs. (4.3) and (4.4) to the first order around some known conditions $\varepsilon^0_{ij}(\vec{p}^0)$, $\eta^0_{ij}(\vec{p}^0)$, we get:

$$\varepsilon_{ij}(\vec{p}) \simeq \varepsilon^0_{ij}(\vec{p}^0) + \sum_{\ell=1}^{L} \left.\frac{\partial \varepsilon_{ij}(p_\ell)}{\partial p_\ell}\right|_{p^0_\ell} (p_\ell - p^0_\ell)$$

$$\text{for all } i,j \tag{4.5}$$

$$\eta_{ij}(\vec{p}) \simeq \eta^0_{ij}(\vec{p}^0) + \sum_{\ell=1}^{L} \left.\frac{\partial \eta_{ij}(p_\ell)}{\partial p_\ell}\right|_{p^0_\ell} (p_\ell - p^0_\ell)$$

$$\text{for all } i,j \tag{4.6}$$

in which L is the total number of parameters to be determined, the superscript "0" denotes a known condition, and $\vec{p}^0 = (p^0_1, p^0_2, \ldots, p^0_L)$, an initial estimate of the unknown parameters which are used to obtain ε^0_{ij} and η^0_{ij} from Eqs. (4.1) and (4.2).

If we seek to minimize the sum of the squares of the errors, then the parameter identification formulation becomes a constrained least-squares minimization problem which can be written as:

$$\text{minimize} \sum_{ij} (\varepsilon^2_{ij} + \eta^2_{ij}) \tag{4.7}$$

subject to:

$$\varepsilon_{ij} = \varepsilon_{ij}^{0}(\vec{p}^{0}) + \sum_{\ell=1}^{L} \left.\frac{\partial \varepsilon_{ij}(p_\ell)}{\partial p_\ell}\right|_{p_\ell^0} (p_\ell - p_\ell^0), \quad \text{for all } i,j \tag{4.8}$$

$$\eta_{ij} = \eta_{ij}^{0}(\vec{p}^{0}) + \sum_{\ell=1}^{L} \left.\frac{\partial \eta_{ij}(p_\ell)}{\partial p_\ell}\right|_{p_\ell^0} (p_\ell - p_\ell^0), \quad \text{for all } i,j \tag{4.9}$$

and

$$p^L \leq p_\ell \leq p^U \quad \text{for all } \ell \tag{4.10}$$

where Eq. (4.10) defines the physical upper and lower bounds (p^U and p^L, respectively) of the parameters. The unknowns in the optimization are ε_{ij}, η_{ij}, for all i,j, and $\vec{p}$. Since the relationships between ε_{ij}, η_{ij} and p_ℓ are not explicitly known, the partial derivatives, $\frac{\partial \varepsilon}{\partial p}$ and $\frac{\partial \eta}{\partial p}$ can only be estimated by finite difference approximations:

$$\frac{\partial \varepsilon_{ij}}{\partial p_\ell} \quad \frac{\Delta \varepsilon_{ij}}{\Delta p_\ell} \quad \text{for all } \ell \tag{4.11}$$

$$\frac{\partial \eta_{ij}}{\partial p_\ell} \quad \frac{\Delta \eta_{ij}}{\Delta p_\ell} \quad \text{for all } \ell \tag{4.12}$$

in which Δp_ℓ is a small independent perturbation of the ℓth parameter, and $\Delta\varepsilon_{ij}$ and $\Delta\eta_{ij}$ are the corresponding changes of errors due to the change in $p_\ell(\Delta p_\ell)$.

Substituting Eqs. (4.8), (4.9), (4.11), and (4.12) into Eq. (4.7), the optimization problem becomes:

$$\text{minimize} \sum_{ij} \left[\varepsilon^0_{ij}(\vec{p}^0) + \sum_{\ell=1}^{L} \left. \frac{\Delta\varepsilon_{ij}}{\Delta p_\ell} \right|_{p^0_\ell} (p_\ell - p^0_\ell) \right]^2$$

$$+ \left[\eta^0_{ij}(\vec{p}^0) + \sum_{\ell=1}^{L} \left. \frac{\Delta\eta_{ij}}{\Delta p_\ell} \right|_{p^0_\ell} (p_\ell - p^0_\ell) \right]^2 \qquad (4.13)$$

$$\text{subject to:} \quad p^L \leq p_\ell \leq p^U \quad \text{for all } \ell \qquad (4.14)$$

Eqs. (4.13) and (4.14) form a standard quadratic programming (QP) problem with 2xL constraints, and L unknowns. The QP problem can be solved by many available software packages. The particular solution method used in this study is introduced later in this chapter.

Note that because of the linearization of the error functions (Eqs. (4.5) and (4.6)), the optimization problem (Eqs. (4.13) and (4.14)) will be solved iteratively from an initial estimate of $\vec{p}^0$ (and ε^0_{ij}, η^0_{ij}), until a convergent solution is obtained. The convergence properties of the proposed algorithm will be demonstrated in two numerical examples given later.

Solution

The PI formulation introduced above was coded in FORTRAN 77 and attached to the original USGS-MOC code with only slight modifications. For convenience,

the combined code is referred to as PI-MOC. The original USGS-MOC code has been modified so that a longitudinal dispersivity (α_L), and a transverse dispersivity (α_T) are now input parameters (instead of having a longitudinal dispersivity and a factor which relate transverse to longitudinal dispersivity). Further, the code has been so modified that the user can choose the particular parameters he wishes to identify. Specifically, for example, the user can choose to identify only transmissivity, or dispersivity coefficients, or both. When identifying transmissivity only, the user can specify that only the flow calculation part of the USGS-MOC code be used (all η's and their expansions are dropped from Eq. (4.13)). The latter modification is for convenience as well as numerical efficiency, as explained below.

In this study, the parameter identification was done in two stages. In the first stage, the PI algorithm was used to identify transmissivities from only the piezometric head observations and the flow calculation part of the USGS-MOC code. With the estimated transmissivity values, the PI algorithm was used again (second stage) with the entire model to find dispersivity coefficients from concentration observations. The reasons for doing so were to ensure efficiency and stability. The majority of the computational requirements in USGS-MOC code are for the solution of the transport equation (particle movement). If head and concentration are used at the same time, then the transport equation must be solved for every parameter perturbation (Eqs. (4.11) and (4.12)). Further, the iterative optimization solution of Eqs. (4.13) and (4.14) converges slowly when head and concentration observations are considered simultaneously. This is a numerical problem caused by the orders-of-magnitude differences between the values of transmissivity (T) and dispersivities (α_L, α_T), and those of $\frac{\Delta\varepsilon}{\Delta p}$ and $\frac{\Delta\eta}{\Delta p}$ when T,

α_L, and α_T are considered together. The primary concern over the use of the two-stage approach is the accuracy of the estimated parameters. This will be investigated in the following numerical examples.

Testing of PI-MOC

A hypothetical aquifer was created to test the effectiveness and efficiency of the combined PI and USGS-MOC (PI-MOC) algorithms. The hypothetical aquifer was 56,000 ft. by 36,000 ft., and had a uniform thickness of 50 ft. The known boundary conditions, the locations of the source, six pumping wells, and 23 observation wells are all shown in Figure 4-1. The pumping schedules used are given in Table 4-1. The aquifer was designed to be characterized by nine different transmissivity zones, as shown in Figure 4-2. The storage coefficient was set to 3×10^{-5}, and porosity to 0.3. The initial head values of the aquifer were obtained from a steady-state solution with the given boundary conditions, but with no pumping. The initial concentration was set to 20 units (USGS-MOC allows the input of any concentration unit the user

Table 4-1. Pumping Schedule for the Test Aquifer.

Well Number[1]	Pumping Rate($ft.^3/s$)
1	3.35
2	2.23
3	1.12
4	3.35
5	2.23

1. See Fig. 1 for their locations

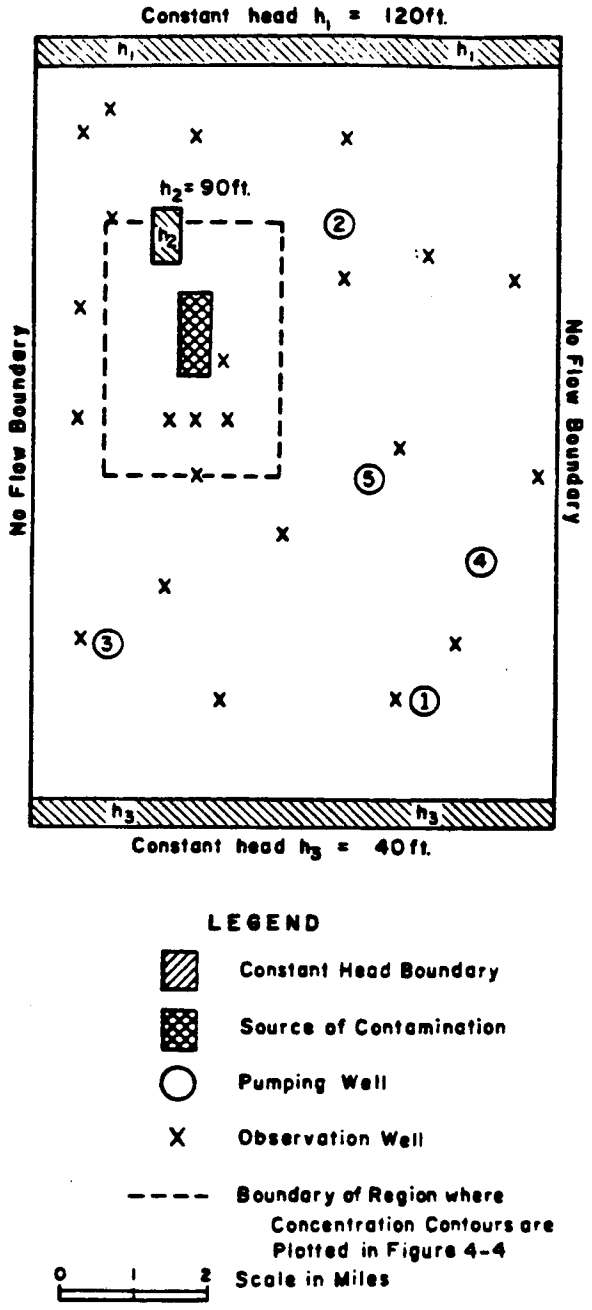

Figure 4-1. A Hypothetical Aquifer for Testing the PI-MOC Algorithm.

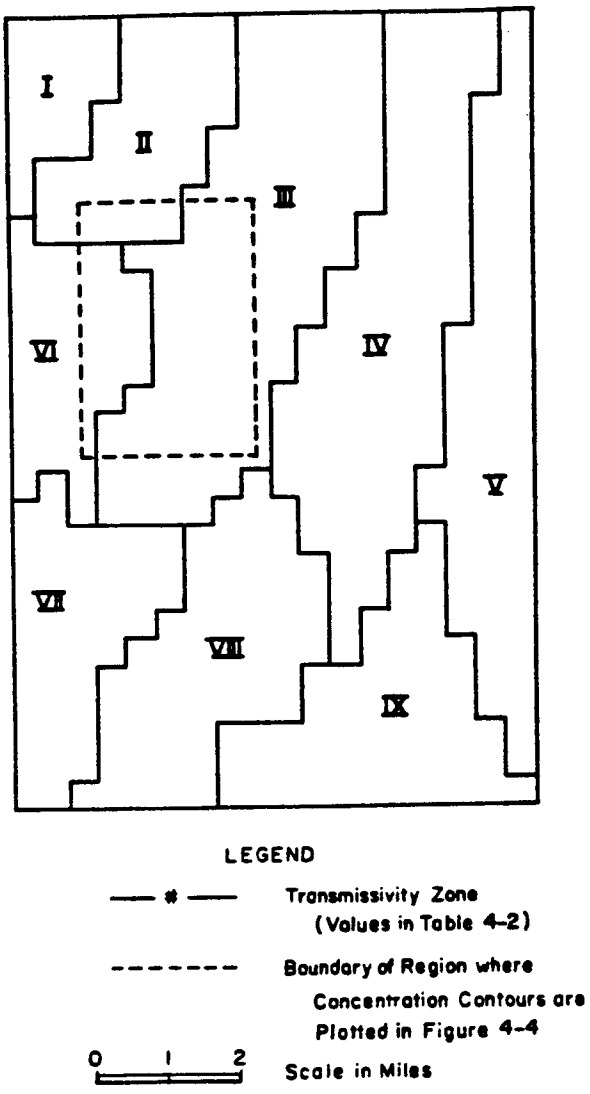

Figure 4-2. Transmissivity Zones of the Hypothetical Aquifer.

desires). The longitudinal and transverse dispersivity coefficients were set to 175 and 70, respectively. The aquifer was isotropic with respect to transmissivity. The concentration of the source was 3000 units.

Using all the known aquifer parameters, the initial condition, and the boundary conditions, the USGS-MOC code was run to generate "observations" of piezometric head and concentration data at the 23 observation wells. Both head and concentration data were available at all the observation wells. Using only these observations, the proposed PI algorithm with the USGS-MOC code was run to uncover the known transmissivities (shown in Table 4-2) and dispersivity coefficients (given above), while assuming that the other parameters and the initial and boundary conditions were all known. The test results are given in two numerical examples below.

Table 4-2. Results of the First Example.

Transmissivity Zone	Transmissivity Found by PI-MOC ($ft.^2/s$)	True Transmissivity ($ft.^2/s$)
1	0.172	0.174
2	0.229	0.231
3	0.290	0.289
4	0.350	0.347
5	0.406	0.405
6	0.201	0.203
7	0.257	0.260
8	0.320	0.318
9	0.383	0.376
Dispersivities		
α_L	173	175
α_T	72	70

Example 1

In the first example, it was assumed that the transmissivity zonation pattern (Fig. 4-2) was known, but not the transmissivity values themselves. Although this assumption was unrealistic, it was essential for verifying the PI-MOC algorithm.

Using only the observations, the optimal parameters found by the PI-MOC algorithm were compared with the true values in Table 4-2. From a uniform initial estimate of 0.1 $ft.^2/s$ for transmissivities in all the zones, four iterations (of solving Eqs. (4.13) and (4.14) without the η terms) were required to reach the listed values which are all within one percent of the true values. The dispersivity coefficients were also found by solving Eqs. (4.13) and (4.14) (but without the ε terms) in four iterations. The results given in Table 4-2 confirm that the proposed PI procedure does accurately recover the selected USGS-MOC model parameters under the rather ideal conditions.

Example 2

In the second example, the same aquifer and observation data were used. However, no knowledge of the zonation pattern of transmissivities was assumed and the aquifer was treated as being homogeneous (characterized by one transmissivity value).

The optimal parameter values found by the PI algorithm in this example are shown in Table 4-3. From Table 4-3, the effect of the simplified characterization of the aquifer on the estimates of dispersivities can be seen. The dispersivities found were much greater than the actual values. The ratio between longitudinal and transverse dispersivity was, however, maintained within nine percent of the actual ratio. The large dispersivities

Table 4-3. Results of the Second Example.

Transmissivity Zone	Transmissivity found by PI-MOC ($ft.^2/s$)	True Transmissivity ($ft.^2/s$)
1	0.273	0.174
2	0.273	0.231
3	0.273	0.289
4	0.273	0.347
5	0.273	0.405
6	0.273	0.203
7	0.273	0.260
8	0.273	0.318
9	0.273	0.376
Dispersivities		
α_L	403	175
α_T	175	70

indicate that with over-simplication of transmissivity characterization, transport due to dispersion was overestimated. To further examine the results of simple characterization, the predicted head and concentration values at the end of the calibration period were plotted against the true head and concentration values (obtained by running the USGS-MOC model with the true parameters) in Figures 4-3 and 4-4. From the contour plots, it can be seen that the differences between the true and the predicted heads are less significant than the differences between the true and the predicted concentrations. This example shows that with a simpler characterization of the aquifer, the algorithm is still able to select a set of parameters that can predict the contaminant plume shape fairly well, but the actual values of concentration at various locations may be less accurate.

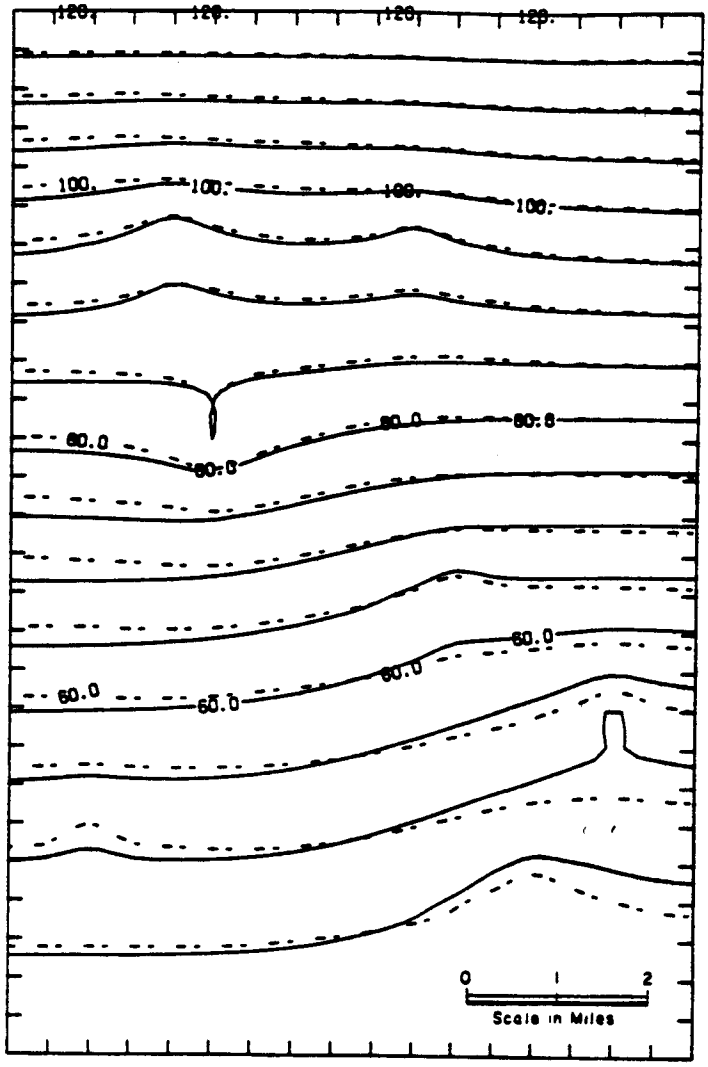

Figure 4-3. Comparison of Actual and Predicted Hydraulic Head Contours from Example 2 (ft.).

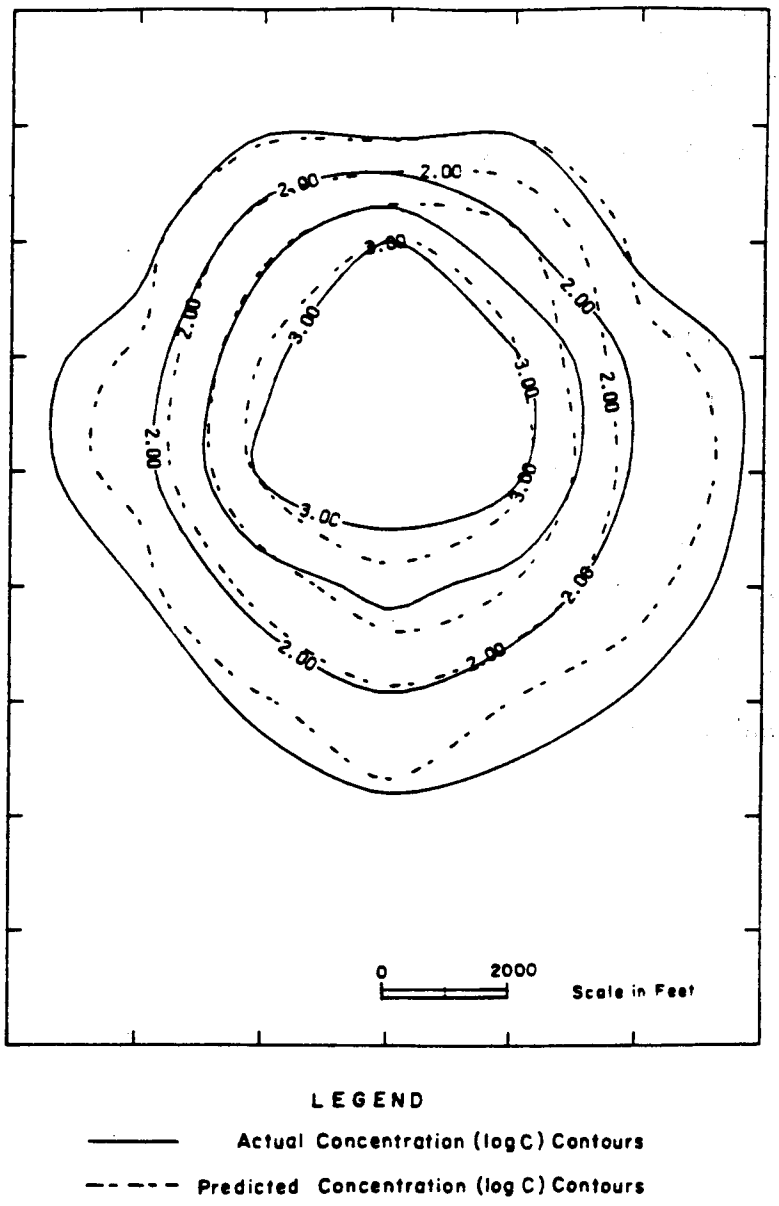

Figure 4-4. Comparison of Actual and Predicted Concentration Contours (Logarithmic Units) from Example 2.

The results from the computational examples show that a parameter identification (PI) algorithm has been successfully combined with the USGS-MOC code. The algorithm has been tested and shown to work accurately and efficiently for two hypothetical situations.

The development of the present PI method was based on an important assumption. The model prediction errors were assumed to be caused only by incorrect aquifer parameter values. The errors from the estimates of initial conditions, boundary conditions, hydraulic and contaminant source information, aquifer thickness, characterization, numerical errors, and measurement noise were ignored in the PI formulation. Incorporating all the possible sources of prediction errors into a PI formulation is not trivial, and work of this nature has not been reported. These other sources of error could lead to significant parameter estimation errors and therefore model production errors.

CHAPTER 5

BLOCK RANDOM FIELD GENERATOR

In the field, perfect data are never available for model calibration. Initial and boundary conditions are never truly known, and localized heterogeneities in aquifer parameters are not accounted for in numerical models of groundwater flow and transport. Therefore, a realistic test of the PI procedure and analysis of data requirements requires that the simulated head and concentration observations reflect the various error sources and micro-heterogeneities in aquifer parameters unaccounted for in model output, but present in the field. To incorporate the data uncertainty into the observations, a random field generator, which preserves spatial and serial correlation, was created. This chapter describes the formulation and testing of this random field generator.

Previous approaches to the parameter or model uncertainty problem have assumed that observations of heads and concentrations are the sum of a deterministic component (model prediction) and a random, statistically independent perturbation component (see for example, Yeh and Yoon, 1976). The assumption that the perturbations are uncorrelated is not reasonable as many of the sources of error are found throughout the aquifer and tend to give data noise that is correlated both spatially and serially. Effects of correlated noise on model calibration have been examined recently by Sadeghipour and Yeh (1984).

When a numerical model is used to produce observation data for calibration, data is produced at many more sites than the number of

observation stations. For instance, in a non-steady-state groundwater flow model, head values may be saved at selected time intervals and at all computational nodes. To add correlated noise to all model output would be computationally expensive if there were a large number of nodes. In past studies, the noise has been added only to specific observations (Yeh and Yoon, 1976; Sadeghipour and Yeh, 1984). If sampling strategies such as number of wells used, well location pattern, and length of the sampling record were to be considered, a new set of noise terms would have to be generated for each change in sampling strategy. The computational requirement would make comparison of sampling strategies nearly impossible.

Various random field generation schemes have been proposed for water resources research. These include the addition of harmonics of random frequencies sampled from the spectral density function (Mejia and Rodriguez-Iturbe, 1974), the turning bands approach (Delhomme, 1979), and an n'th order nearest neighbor model (Whittle, 1963). The last model was applied by Smith and Freeze (1979a, b). All of these schemes are somewhat limited by the number of spatial nodal values which can be produced efficiently. The scheme presented here is capable of creating a large set of spatially and serially correlated noise terms efficiently and accurately. Noise terms created by the method we propose are added to observations in order to reflect model and data uncertainty.

Generating Model

Because no information is available on the correlation structure of model versus observation residuals following Mejia and Rodriguez-Iturbe (1974), the assumption of time-space separability is made:

$$\zeta(x,t) = \alpha(x)\beta(t) \tag{5.1}$$

where ζ, α, and β are zero mean processes, $\alpha(x)$ is time-independent, and $\beta(t)$ is spatially independent. In general, the problem addressed is the generation of a random field over a uniform grid, where the spatial correlation structure is an arbitrary function $\alpha(x)$, where x is the location separation vector, and the spatial correlation function is therefore homogeneous. The temporal correlation function is assumed to be of a lag one Markov form, $\rho(t+1) = \rho(t)$. The method described could be generalized to more complex forms (e.g., n'th order auto-correlation models), however, in most hydrologic applications, record lengths are not long enough to allow identification of more complex models, so the lag one Markov correlation structure is preferred.

If one were interested only in generating a multivariate synthetic lag one Markov sequence at N locations, with the same lag one correlation coefficient at all sites, but with arbitrary spatial correlation between the sites, a simple generation scheme could be used:

$$\vec{Y}_t = A\vec{Y}_{t-1} + B\vec{E}_t \tag{5.2a}$$

where $A = \rho I$ (5.2b)

and $BB^T = (1-\rho^2)P$ (5.2c)

where P is the NxN spatial correlation matrix of the observations, E is an Nx1 vector of standard (mean zero, variance one) independent normal random deviates, A and B are NxN coefficient matrices to be computed, and ρ is the constant (over the domain) serial correlation coefficient. A solution for B satisfying Eq. (5.2c) can be found using a suitable matrix decomposition method (Matalas, 1967). In this work, a Choleski decomposition, as recommended by Salas et al. (1980) was used.

While such an approach is conceptually trivial, it has a major disadvantage in application to generation of random fields when the N sites correspond to N computational nodes. In the case of a groundwater model, N can be quite large (typically greater than 400). Decomposition and multiplication of such large matrices would be difficult, or at best, very inefficient. A computationally more efficient algorithm would therefore be desirable.

If the computational grid is uniform, or can be approximated uniform (for instance, by ignoring 'imaginary' locations outside a physical boundary), a much more efficient approach is possible. Consider the rectangular uniform grid shown in Figure 5-1, which is subdivided into rectangular blocks as shown. Then the proposed generating equation is:

$$\vec{Y}_{t,n} = A\vec{Y}_{t-1,n} + B\vec{E}_{t,n} + C\vec{Y}_{t,n-1} + D\vec{Y}_{t,n-b} \qquad (5.3)$$

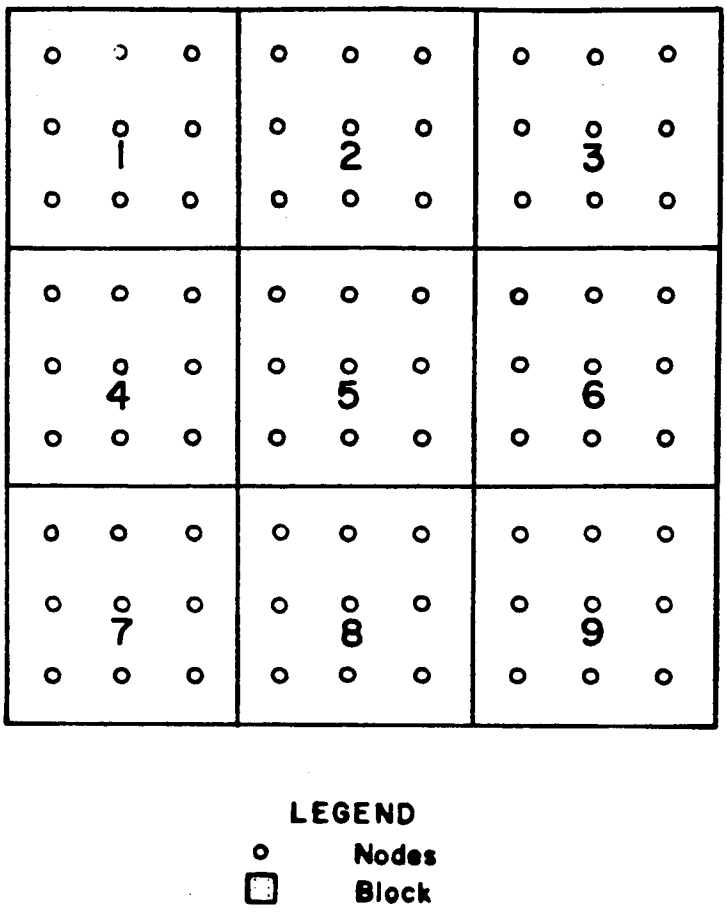

Figure 5-1. Sub-division of a Region into Blocks for Block Random Field Generator.

where A,B,C, and D are MxM matrices, M is the number of nodes in each block, n is the block index, and b is the number of blocks in a row of the grid. The matrix A preserves the serial correlation of the generated observations, C and D maintain the spatial correlation with adjacent blocks, and B maintains the spatial correlation within the block being generated. The spatial correlation between blocks which are not adjacent is assumed to be preserved implicitly (an assumption that will later be verified). The major advantage of this formulation is that multiple computations (at each time step) involving MxM matrices replace single computations involving NxN matrices.

Using the following definitions,

$$E(\vec{Y}_{t,n}, \vec{Y}^{T}_{t-1,n}) = T = \rho P \tag{5.4a}$$

$$E(\vec{Y}_{t,n}, \vec{Y}^{T}_{t,n}) = P \tag{5.4b}$$

$$E(\vec{Y}_{t,n}, \vec{Y}^{T}_{t,n-1}) = P_1 \tag{5.4c}$$

$$E(\vec{Y}_{t,n}, \vec{Y}^{T}_{t,n-b}) = P_2 \tag{5.4d}$$

$$E(\vec{Y}_{t,n-1}, \vec{Y}^{T}_{t,n-b}) = P_3 \tag{5.4e}$$

and Eq. (5-3), the following set of equations,

$$T = AP + C\rho P_1^{T} + D\rho P_2^{T} \tag{5.5a}$$

$$P_1 = A\rho P_1 + CP + DP_3T \tag{5.5b}$$

$$P_2 = A\rho P_2 + CP_3 + DP \tag{5.5c}$$

$$P = \rho AP + BB^T + CP_1{}^T + DP_2{}^T \tag{5.5d}$$

can be solved to find A, BB^T, C, and D, with

$$A = \rho[P-M_1-M_2*M_3*M_4]*[P-\rho^2*M_1-\rho^2*M_2*M_3*M_4]^{-1} \tag{5.6}$$

$$C = [(I-A\rho)*M_2]*M_3{}^{-1} \tag{5.7}$$

$$D = [(I-A\rho)P_2 - CP_3]*P^{-1} \tag{5.8}$$

$$BB^T = P - \rho AP - CP_1{}^T - DP_2{}^T \tag{5.9}$$

where * is used as a matrix multiplication sign, and

$$M_1 = P_2\ P^{-1}P_2{}^T \tag{5.10a}$$

$$M_2 = P_1 - P_2\ P^{-1}P_3{}^T \tag{5.10b}$$

$$M_3 = [P - P_3\ P^{-1}P_3{}^T]^{-1} \tag{5.10c}$$

$$M_4 = P_1 - P_3\ P_1{}^{-1}P_2{}^T \tag{5.10d}$$

BB^T is decomposed to find B by the Choleski decomposition method. When a block is generated which is either in the first row or the first column (with the exception of block 1), the generation equation is

$$\vec{Y}_{t,n} = A\vec{Y}_{t,n} + B\vec{E}_{t,n} + C\vec{Y}_{t,n-c} \tag{5.11}$$

where C is the number of blocks in a row if the generated block is in column 1, and is equal to one if the generated block is in row 1. With the above definitions, A, BB^T, and C are then:

$$A = \rho[P - P_1 P^{-1} P_1^T]*[P - \rho^2 P_1 P^{-1} P_1^T]^{-1} \tag{5.12}$$

$$C = [P_1 - A\rho P_1]*[P]^{-1} \tag{5.13}$$

$$BB^T = P - \rho AP - CP_1^T \tag{5.14}$$

where P_1 is now the spatial correlation matrix which preserves correlation between the current block and a neighboring block.

The scheme of this generator is to first generate spatially correlated terms in block one (Fig. 5-1), and create "one block" correlation for the rest of the first row (blocks 2 and 3, Fig. 5-1) from Eq. (5.9). The process then moves to the second row and creates "one block" correlation for the first block in that row (block 4). The rest of the blocks (blocks 5 and 6) in the second row are made spatially correlated from Eq. (5.3) with the block above it and the block generated previously in that row. (This is called "two

block" correlation.) This process continues row by row until a field at one time step is completed. At each time step, the blocks are also made lag one serially correlated with the previous time step. The intention of this method is that by maintaining correlations explicitly between adjacent blocks as they are generated, spatial correlation is implicitly maintained between blocks that are not adjacent.

Test Results of Block Random Multivariate Generator

To test the generator, random numbers with mean zero and variance one were generated at each of the nodes shown in Figure 5-1. The spatial correlation matricies (P, P_1, P_2, and P_3) were defined by a function which decays with distance between nodes, as described by Rodriguez-Iturbe and Mejia (1974):

$$r_{ij}(\nu_{ij}) = b\nu_{ij}K_1(b\nu_{ij}) \tag{5.15}$$

Where r_{ij} is the correlation between points i and j, ν_{ij} is the distance between points i and j, b is a parameter to define the desired spatial correlation, and K_1 is a modified Bessel function. The above equation was used because it was felt to be a more realistic decaying function than an exponential decaying function. Exponential decaying functions are 'too continuous' to be realistic (Matern, 1960). Both correlation curves are monotonically decreasing, but the modified Bessel decaying function has a slower rate of decay than the exponential decaying function (Whittle, 1954).

For the test of the generator at one nodal distance away (straight across or down), a spatial correlation of 0.90 (b = 0.90) was used to define the decaying Bessel function. In this test, the serial correlation was specified to be zero, as the implicit preservation of spatial correlation was the desired result of the generator.

Twenty-100-time step sequences were generated, and spatial correlations between chosen blocks were calculated. Figure 5-2 shows the plot of correlation with unit distance between nodes for block 1, which is explicitly correlated in the scheme. Figures 5-3 through 5-6 show the correlation structure between blocks (not including correlation among nodes in any one block) which are never explicitly correlated (blocks which are not adjacent) in the scheme.

By observing the results shown in Figures 5-3 to 5-6, it is apparent that the generator successfully produced a field of random numbers whose spatial correlation structure throughout the entire domain is quite similar to the theoretical spatial correlation structure, which is preserved explicitly only within each block and with adjacent blocks.

A Block Random Multivariate Generator has been presented in this chapter. The proposed generator preserves the lag zero spatial correlation and lag one serial correlation for the entire random field. It implicitly retains the spatial correlation structure. The generator is computationally efficient and does not require large computer memory. The generator was used to add uncertainty to the observation data, as described in Chapter 6.

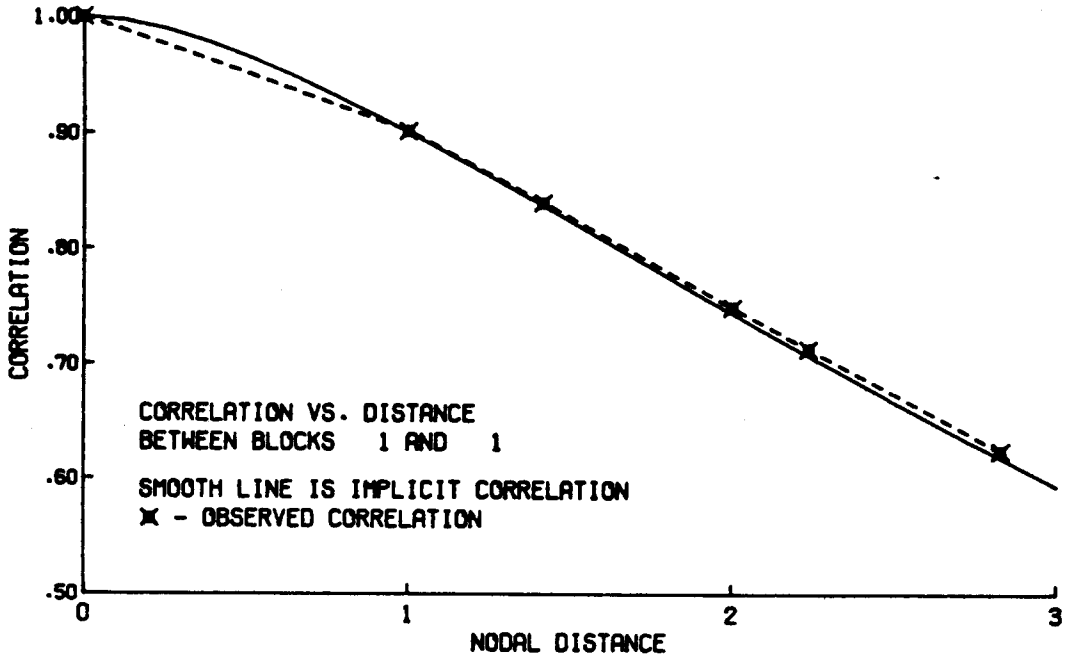

Figure 5-2. Correlation Versus Nodal Distance, Comparing Specified and Observed Correlation for Nodes in Block 1 (Figure 5-1).

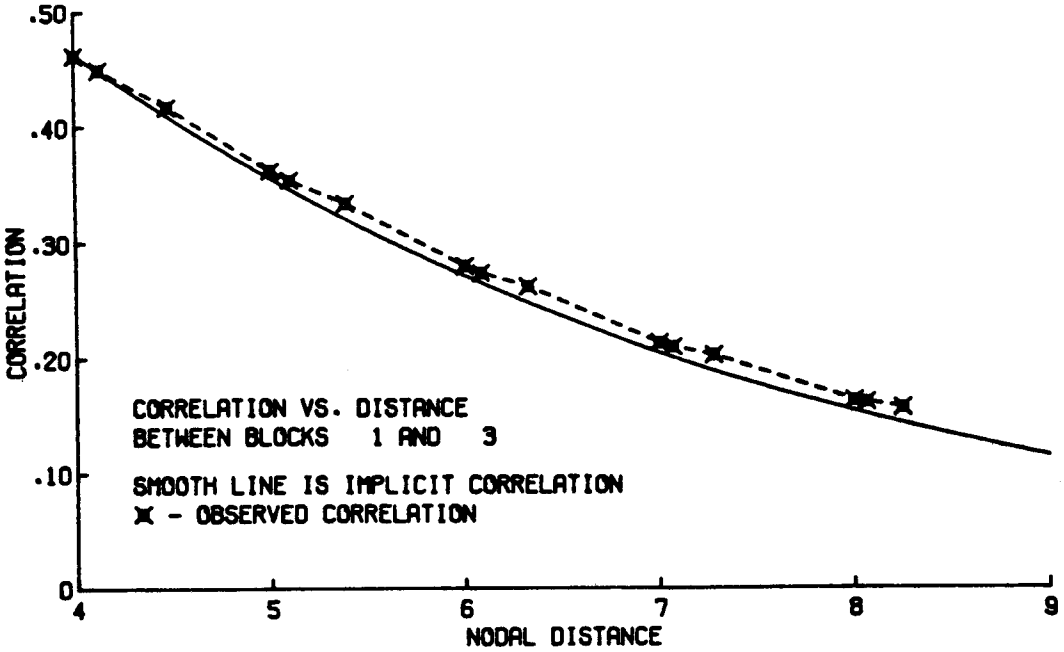

Figure 5-3. Comparison of Implied and Observed Correlation Between Nodes in Blocks 1 and 3 (Figure 5-1).

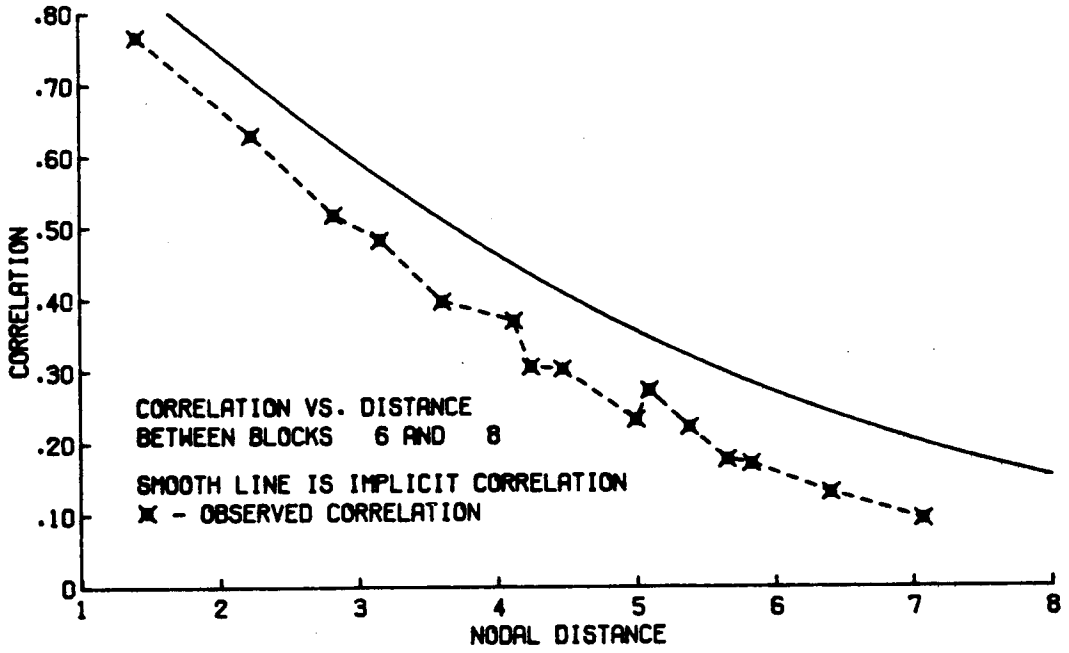

Figure 5-4. Comparison of Implied and Observed Correlation Between Nodes in Blocks 6 and 8 (Figure 5-1).

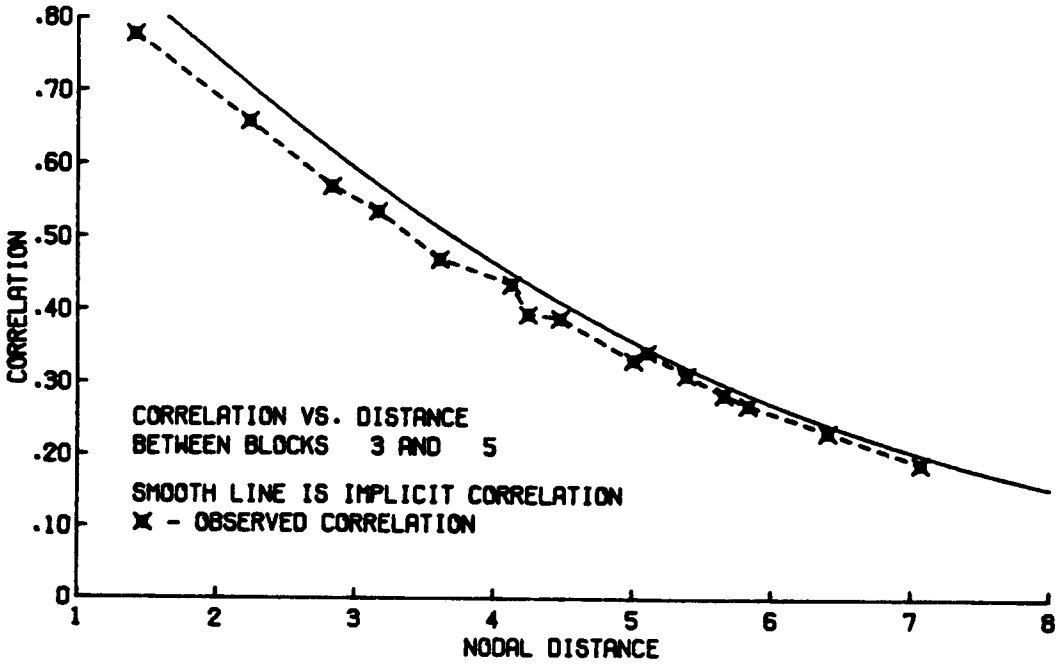

Figure 5-5. Comparison of Implied and Observed Correlation Between Nodes in Blocks 3 and 5 (Figure 5-1).

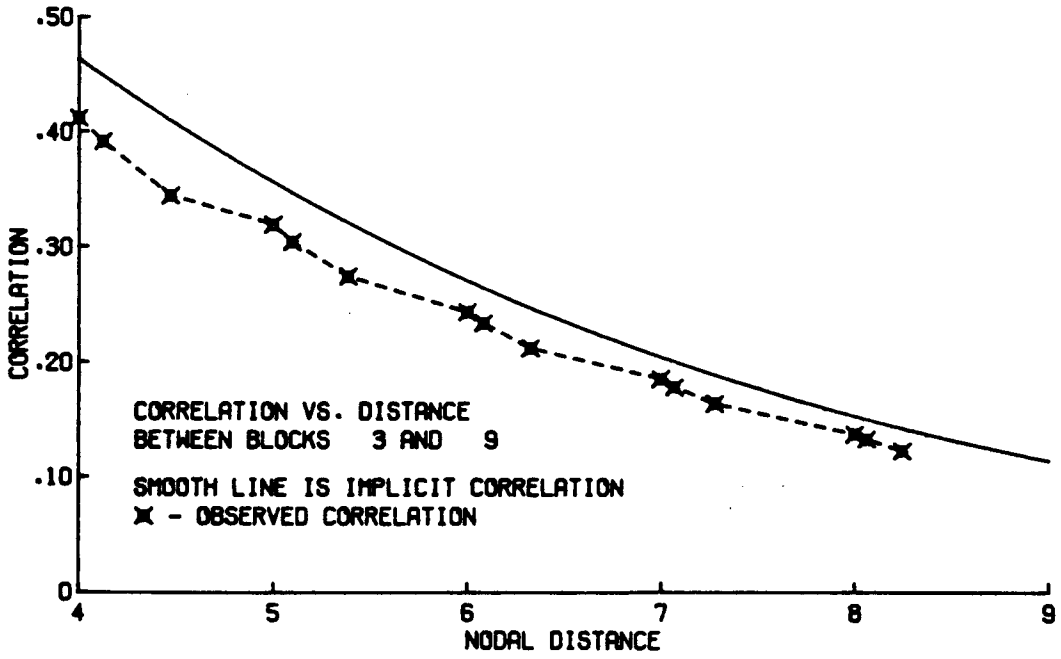

Figure 5-6. Comparison of Implied and Observed Correlation Between Nodes in Blocks 3 and 9 (Figure 5-1).

CHAPTER 6

DESIGN OF EXPERIMENTS

The design of the synthetic aquifer and the numerical experiments are presented in this chapter. In order to achieve the goal of studying the data requirement issue in a realistic setting, the hypothetical aquifer was synthesized by a colleague, Margaret Michalek, without any participation from the investigators. Except for the limited samples, the actual parameters used in the creation of the aquifer were not known to the investigators until all the planned calibration efforts of the aquifer were completed. Following is a description of the synthetic aquifer, the data that was available to the investigators, the data uncertainty levels investigated, and the sampling strategies tested.

Synthetic Aquifer Description

The aquifer configuration and the boundary conditions are shown in Figure 6-1. The contaminant source area had a given constant head node of 540 ft. The source concentration at this node was 5000 units. All other node cells had a background concentration of two units at the beginning of the simulation. The storage coefficient was .00001 and porosity was .20. The distance between nodes in both the x and y directions was 1000 ft.

Selected observations of aquifer thickness and initial water table are given in Table 6-1. The pumping schedule and point estimates of transmissivity at 12 locations are shown in Table 6-2. These data are taken

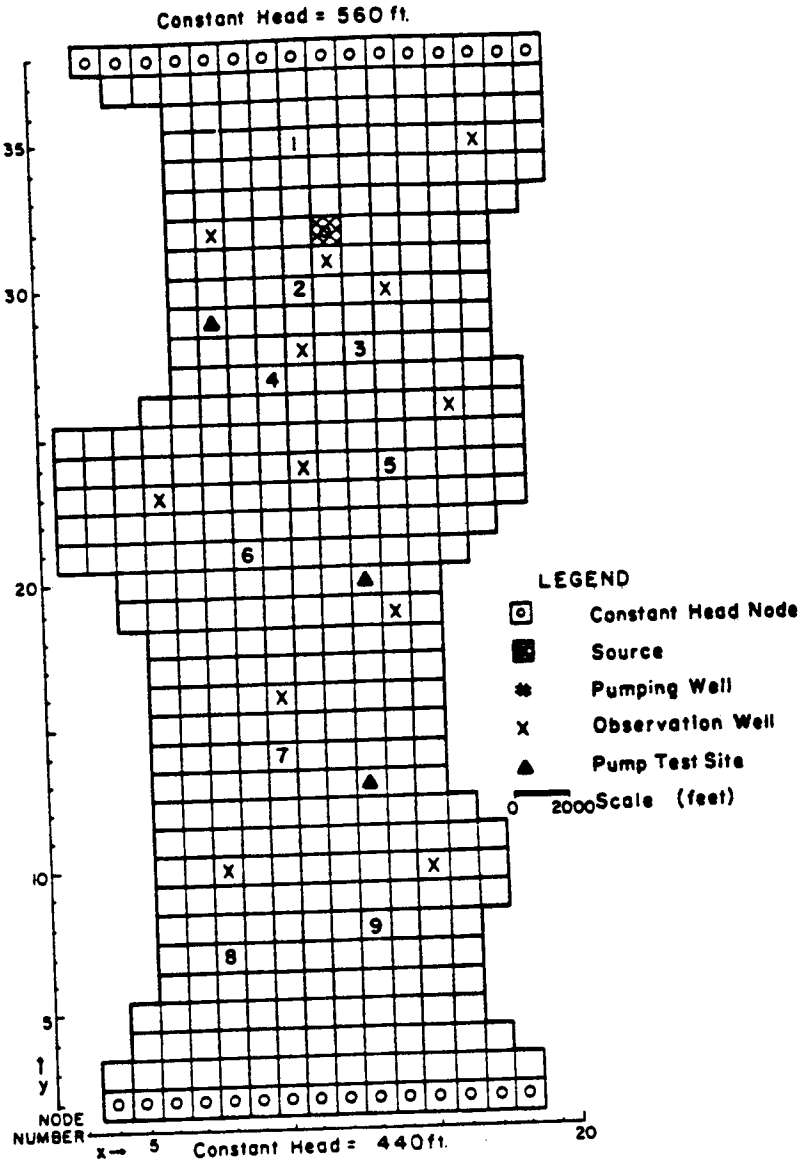

Figure 6-1. Description of Synthetic Aquifer.

Table 6-1. Aquifer Thickness and Initial Water Table Elevation Data Available for Calibration Effort.

	No.	Well Location (x,y)	Confining Layer Thickness (A)	Initial Water Table Elevation (ft.)
Pump Well Locations	1	(11,35)	112	550
	2	(11,40)	106	534
	3	(13,28)	113	528
	4	(10,27)	113	524
	5	(14,24)	108	516
	6	(9,21)	110	504
	7	(10,14)	111	478
	8	(8,7)	97	455
	9	(13,8)	94	458
Three Pump Test Sites		(13,13)	44	475
		(8,29)	68	530
		(13,20)	114	501
Observation Wells		(17,35)	82	553
		(12,31)	113	536
		(14,30)	114	532
		(11,28)	114	524
		(16,26)	75	522
		(11,24)	113	515
		(6,23)	52	509
		(14,19)	109	498
		(10,16)	115	485
		(8,10)	110	465
		(15,10)	73	463

Table 6-2. Pumping Schedule and Point Estimates of Transmissivity Available from Pump Test Data.

Location (x,y)	Pumping Well No.	Pumping Data (CFS)	T ($ft.^2/s$)
(11,35)	1	0.10	0.8
(11,40)	2	0.50	0.9
(13,28)	3	1.00	1.0
(10,27)	4	0.75	1.0
(14,24)	5	1.20	0.75
(19,21)	6	1.40	0.85
(10,14)	7	0.50	1.0
(8,7)	8	0.50	0.7
(13,8)	9	0.50	0.9
Three Pump Test Sites*			
(13,13)	———	———	1.0
(8,29)	———	———	0.4
(13,20)	———	———	0.3

* These three locations contain transmissivity data determined from earlier pump tests.

from the designed hypothetical aquifer. All of the above information presented was known at the beginning of the experiment.

Although it was somewhat unrealistic that much of the above information, such as boundary conditions, source concentration, porosity, and storage coefficient was known, it was given to limit the computational scope of this study. Calibration for these parameters, in addition to the selected transmissivities and dispersivities, presented a much bigger problem.

For the benefit of the readers, the actual aquifer thickness, the initial head distribution, and the actual transmissivity distribution constructed by our enlisted geohydrologist are shown in Figures 6-2, 6-3, and 6-4, respectively. The actual longitudinal and transverse dispersivities were 100 feet and 70 feet, respectively. The dispersivity values and the data shown in Figures 6-2, 6-3, and 6-4 were kept from the investigators until the end of the study.

Using the chosen parameters, five years of monthly (using 30.25 days per month) head and concentration values were generated at each node by the USGS-MOC model. These values were retained by the geohydrologist, but were available for sampling. The sampling was done by a separate software which avoided direct access to the generated data from the investigators. For presentation purposes, the generated head distribution at the end of the fifth year and the contaminant plume at the end of the second, third, fourth, and fifth years are shown in Figures 6-5 and 6-6. The hydraulic heads in this aquifer reached steady-state conditions within two months of changing the pumping schedule.

0. 0. 0. 0. 0. 0. 0. 0. 0. 0. 0. 0. 0. 0. 0. 0. 0. 0. 0. 0. 0.
0. 0. 0. 36. 43. 61. 62. 73. 98.113.113.111.114.110. 95. 74. 60. 44. 39. 0.
0. 0. 0. 0. 36. 52. 65. 77. 98.113.112.110.111.114. 98. 66. 62. 59. 43. 0.
0. 0. 0. 0. 0. 0. 52. 61. 80.112.114.111.114.111. 95. 56. 51. 41. 34. 0.
0. 0. 0. 0. 0. 0. 51. 63. 91.114.112.113.112.113.110. 94. 82. 61. 45. 0.
0. 0. 0. 0. 0. 0. 50. 70. 91.109.113.115.112.114.109. 98. 91. 56. 42. 0.
0. 0. 0. 0. 0. 0. 53. 63. 99.108.113.115.113.115.110. 99. 60. 46. 0. 0.
0. 0. 0. 0. 0. 0. 52. 77. 97. 95.114.110.114.111.107. 99. 75. 0. 0. 0.
0. 0. 0. 0. 0. 0. 53. 81. 97. 96.108.113.113.111.108. 94. 54. 0. 0. 0.
0. 0. 0. 0. 0. 0. 52. 60. 93. 98.106.113.113.114.106. 97. 57. 0. 0. 0.
0. 0. 0. 0. 0. 0. 51. 68. 97.108.111.115.111.111.100. 92. 63. 0. 0. 0.
0. 0. 0. 0. 0. 0. 54. 77. 92.106.114.110.113.111. 97. 98. 71. 0. 0. 0.
0. 0. 0. 0. 0. 0. 62. 77.114.113.111.112.112.106.100. 98. 91. 63. 0. 0.
0. 0. 0. 0. 0. 60. 76. 95.108.111.112.110.110.107. 96. 95. 69. 60. 0. 0.
0. 0. 51. 56. 63. 71. 89. 96.107.110.115.111.114.106. 97. 87. 68. 58. 0. 0.
0. 0. 59. 71. 82. 95. 97. 98.108.113.113.112.114.108. 93. 84. 70. 57. 0. 0.
0. 0. 34. 44. 58. 52. 56. 90.108.115.115.111.112.108. 59. 52. 48. 43. 0. 0.
0. 0. 41. 55. 61. 77. 86.100.110.111.113.111.111.105. 92. 82. 68. 0. 0. 0.
0. 0. 45. 54. 57. 65. 71. 98.110.111.113.111.115.107. 93. 77. 0. 0. 0. 0.
0. 0. 0. 0. 57. 66. 84. 99.106.110.114.112.114.107. 82. 0. 0. 0. 0. 0.
0. 0. 0. 0. 55. 61. 86. 98.108.115.113.111.110.109. 91. 0. 0. 0. 0. 0.
0. 0. 0. 0. 0. 70. 81. 93.113.114.113.113.110. 91. 85. 0. 0. 0. 0. 0.
0. 0. 0. 0. 0. 68. 82. 95.112.113.114.110.112. 94. 75. 0. 0. 0. 0. 0.
0. 0. 0. 0. 0. 64. 86.100.113.115.112.113. 93. 70. 65. 0. 0. 0. 0. 0.
0. 0. 0. 0. 0. 66. 83. 93.114.113.112.114. 98. 77. 64. 0. 0. 0. 0. 0.
0. 0. 0. 0. 0. 72. 97.111.115.111.114. 97. 93. 85. 76. 0. 0. 0. 0. 0.
0. 0. 0. 0. 0. 70. 99.113.110.112.113.100. 94. 80. 74. 0. 0. 0. 0. 0.
0. 0. 0. 0. 0. 72. 99.110.111.111.110.100. 96. 80. 74. 60. 0. 0. 0. 0.
0. 0. 0. 0. 0. 72. 95.112.111.111.111. 96. 96. 91. 70. 69. 58. 0. 0. 0.
0. 0. 0. 0. 0. 73. 99.110.106.107. 98. 98. 95. 92. 82. 74. 68. 0. 0. 0.
0. 0. 0. 0. 0. 71. 93.108. 98.107. 99. 98. 94. 92. 89. 79. 76. 0. 0. 0.
0. 0. 0. 0. 0. 66. 91. 96. 99. 99. 97. 98. 94. 92. 77. 64. 0. 0. 0. 0.
0. 0. 0. 0. 0. 66. 89. 97.100. 98. 98. 97. 94. 91. 73. 70. 0. 0. 0. 0.
0. 0. 0. 0. 0. 60. 83. 99. 99. 98. 96. 95. 93. 92. 76. 75. 0. 0. 0. 0.
0. 0. 0. 0. 52. 66. 88. 97.100. 98. 97. 94. 93. 92. 87. 79. 0. 0. 0. 0.
0. 0. 0. 0. 55. 61. 86. 92. 96. 98. 96. 95. 94. 91. 91. 86. 63. 0. 0. 0.
0. 0. 0. 52. 60. 72. 89. 92. 94. 97. 97. 96. 93. 92. 92. 93. 77. 61. 0. 0.
0. 0. 0. 55. 69. 72. 89. 91. 99. 97. 97. 93. 94. 93. 90. 91. 83. 73. 0. 0.
0. 0. 0. 0. 0. 0. 0. 0. 0. 0. 0. 0. 0. 0. 0. 0. 0. 0. 0. 0. 0.

Figure 6-2. Thickness Map of Synthetic Aquifer (ft.).

0. 0. 0. 0. 0. 0. 0. 0. 0. 0. 0. 0. 0. 0. 0. 0. 0. 0. 0.
0. 0. 0.560.560.560.560.560.560.560.560.560.560.560.560.560.560.560. 0.
0. 0. 0. 0.560.559.558.558.557.557.557.557.558.558.558.558.558.558.558. 0.
0. 0. 0. 0. 0. 0.555.555.554.555.554.555.555.556.556.555.556.556.556. 0.
0. 0. 0. 0. 0. 0.551.551.551.551.551.551.552.552.553.553.553.554.554. 0.
0. 0. 0. 0. 0. 0.548.548.548.547.547.547.547.548.549.550.551.552.553. 0.
0. 0. 0. 0. 0. 0.544.544.544.543.544.543.544.545.546.546.548.550. 0. 0.
0. 0. 0. 0. 0. 0.540.540.540.540.540.540.540.541.542.543.543. 0. 0. 0.
0. 0. 0. 0. 0. 0.537.537.537.537.537.537.537.537.538.539.539. 0. 0. 0.
0. 0. 0. 0. 0. 0.534.534.534.534.534.534.534.534.534.535.535. 0. 0. 0.
0. 0. 0. 0. 0. 0.530.530.530.530.531.531.531.530.531.531.531. 0. 0. 0.
0. 0. 0. 0. 0. 0.526.526.526.527.528.528.528.527.528.528.528. 0. 0. 0.
0. 0. 0. 0. 0. 0.522.522.523.524.525.525.525.525.525.525.525.523. 0. 0.
0. 0. 0. 0. 0.514.517.519.520.521.522.523.523.523.523.522.522.522. 0. 0.
0. 0.509.510.510.512.514.515.517.517.519.519.520.520.520.520.520.520. 0. 0.
0. 0.509.509.510.511.512.512.513.514.515.515.516.516.517.517.518.519. 0. 0.
0. 0.508.508.508.509.509.510.510.510.511.512.512.513.514.515.516.517. 0. 0.
0. 0.507.507.507.506.506.507.507.507.508.508.509.510.511.513.514. 0. 0. 0.
0. 0.507.506.505.504.504.503.504.504.504.505.506.506.507.510. 0. 0. 0. 0.
0. 0. 0. 0.502.501.501.500.500.500.500.501.501.502.502. 0. 0. 0. 0. 0.
0. 0. 0. 0.500.498.497.497.496.496.497.497.497.498.498. 0. 0. 0. 0. 0.
0. 0. 0. 0. 0.493.493.493.493.493.493.493.493.494.494. 0. 0. 0. 0. 0.
0. 0. 0. 0. 0.489.489.489.489.489.489.489.489.490.490. 0. 0. 0. 0. 0.
0. 0. 0. 0. 0.485.485.485.485.485.485.485.486.486.486. 0. 0. 0. 0. 0.
0. 0. 0. 0. 0.482.481.481.481.481.481.481.482.482.482. 0. 0. 0. 0. 0.
0. 0. 0. 0. 0.478.478.478.478.478.478.478.478.478.478. 0. 0. 0. 0. 0.
0. 0. 0. 0. 0.475.475.475.476.476.476.475.475.475.474. 0. 0. 0. 0. 0.
0. 0. 0. 0. 0.472.472.472.473.473.473.472.471.471.469.467. 0. 0. 0. 0.
0. 0. 0. 0. 0.468.468.469.469.469.469.468.468.467.466.465.464. 0. 0. 0.
0. 0. 0. 0. 0.465.465.465.465.465.465.465.464.464.463.463.463. 0. 0. 0.
0. 0. 0. 0. 0.462.462.462.462.462.462.461.461.461.461.461.462. 0. 0. 0.
0. 0. 0. 0. 0.458.458.459.458.458.458.458.458.458.457.458. 0. 0. 0. 0.
0. 0. 0. 0. 0.455.455.455.455.455.455.455.455.455.455.455. 0. 0. 0. 0.
0. 0. 0. 0. 0.451.452.451.451.451.452.452.452.452.452.452. 0. 0. 0. 0.
0. 0. 0. 0.446.448.448.448.448.448.448.448.448.449.449.448. 0. 0. 0. 0.
0. 0. 0. 0.444.445.445.445.445.445.445.445.445.445.445.443. 0. 0. 0.
0. 0. 0.441.442.442.442.443.442.442.442.442.442.442.443.442.442.441. 0. 0.
0. 0. 0.440.440.440.440.440.440.440.440.440.440.440.440.440.440.440. 0. 0.
0. 0. 0. 0. 0. 0. 0. 0. 0. 0. 0. 0. 0. 0. 0. 0. 0. 0. 0. 0. 0.

Figure 6-3. Initial Hydraulic Heads of Synthetic Aquifer (ft.).

.00 .00 .00 .00 .00 .00 .00 .00 .00 .00 .00 .00 .00 .00 .00 .00 .00 .00 .00 .00
.00 .00 .00 .27 .41 .45 .58 .69 .91 .82 .90 .861.15 .84 .88 .65 .47 .35 .27 .00
.00 .00 .00 .00 .25 .39 .43 .53 .66 .89 .861.13 .88 .91 .83 .58 .53 .49 .27 .00
.00 .00 .00 .00 .00 .00 .42 .37 .61 .891.15 .84 .78 .69 .86 .54 .39 .36 .39 .00
.00 .00 .00 .00 .00 .00 .35 .30 .73 .50 .83 .74 .41 .36 .53 .56 .52 .42 .37 .00
.00 .00 .00 .00 .00 .00 .35 .42 .69 .51 .89 .78 .46 .43 .45 .47 .37 .38 .27 .00
.00 .00 .00 .00 .00 .00 .35 .35 .37 .86 .86 .87 .76 .42 .38 .45 .35 .38 .00 .00
.00 .00 .00 .00 .00 .00 .42 .43 .47 .87 .891.11 .69 .41 .41 .43 .30 .00 .00 .00
.00 .00 .00 .00 .00 .00 .41 .39 .57 .86 .81 .89 .87 .38 .38 .43 .34 .00 .00 .00
.00 .00 .00 .00 .00 .00 .35 .44 .38 .83 .891.12 .73 .46 .44 .36 .22 .00 .00 .00
.00 .00 .00 .00 .00 .00 .25 .41 .39 .891.151.10 .82 .44 .35 .36 .42 .00 .00 .00
.00 .00 .00 .00 .00 .00 .30 .34 .37 .841.15 .821.15 .88 .46 .35 .39 .00 .00 .00
.00 .00 .00 .00 .00 .00 .30 .30 .881.11 .90 .90 .811.15 .46 .43 .41 .38 .00 .00
.00 .00 .00 .00 .00 .27 .30 .50 .84 .81 .84 .81 .831.13 .44 .38 .44 .35 .00 .00
.00 .00 .41 .43 .41 .49 .56 .53 .90 .74 .42 .37 .43 .75 .44 .38 .45 .35 .00 .00
.00 .00 .45 .44 .49 .46 .64 .65 .86 .72 .44 .35 .46 .75 .31 .41 .37 .28 .00 .00
.00 .00 .39 .38 .35 .37 .52 .58 .78 .74 .38 .34 .751.13 .31 .38 .38 .28 .00 .00
.00 .00 .38 .39 .45 .37 .53 .49 .91 .76 .46 .39 .741.10 .29 .44 .45 .00 .00 .00
.00 .00 .37 .38 .37 .42 .56 .50 .84 .73 .32 .35 .36 .84 .29 .38 .00 .00 .00 .00
.00 .00 .00 .00 .38 .38 .53 .56 .83 .72 .49 .46 .30 .88 .44 .00 .00 .00 .00 .00
.00 .00 .00 .00 .38 .36 .43 .46 .82 .78 .37 .32 .84 .84 .34 .00 .00 .00 .00 .00
.00 .00 .00 .00 .00 .34 .42 .52 .81 .79 .37 .46 .83 .56 .31 .00 .00 .00 .00 .00
.00 .00 .00 .00 .00 .44 .37 .51 .91 .79 .41 .46 .86 .53 .32 .00 .00 .00 .00 .00
.00 .00 .00 .00 .00 .39 .42 .53 .84 .76 .37 .57 .82 .57 .31 .00 .00 .00 .00 .00
.00 .00 .00 .00 .00 .46 .44 .46 .87 .75 .38 .69 .71 .51 .34 .00 .00 .00 .00 .00
.00 .00 .00 .00 .00 .41 .52 .871.131.15 .78 .76 .73 .46 .31 .00 .00 .00 .00 .00
.00 .00 .00 .00 .00 .46 .58 .801.151.15 .80 .781.15 .52 .30 .00 .00 .00 .00 .00
.00 .00 .00 .00 .00 .46 .56 .83 .87 .88 .37 .42 .82 .46 .27 .38 .00 .00 .00 .00
.00 .00 .00 .00 .00 .51 .52 .87 .39 .74 .38 .39 .82 .57 .42 .50 .39 .00 .00 .00
.00 .00 .00 .00 .00 .45 .62 .90 .46 .78 .44 .41 .83 .53 .50 .44 .39 .00 .00 .00
.00 .00 .00 .00 .00 .44 .89 .88 .36 .76 .44 .45 .88 .76 .39 .47 .36 .00 .00 .00
.00 .00 .00 .00 .00 .44 .73 .69 .36 .73 .35 .37 .88 .79 .39 .51 .00 .00 .00 .00
.00 .00 .00 .00 .00 .53 .80 .69 .36 .72 .45 .72 .87 .78 .65 .46 .00 .00 .00 .00
.00 .00 .00 .00 .00 .64 .71 .74 .39 .73 .43 .41 .71 .52 .64 .46 .00 .00 .00 .00
.00 .00 .00 .00 .37 .51 .80 .84 .36 .79 .36 .45 .82 .56 .43 .43 .00 .00 .00 .00
.00 .00 .00 .00 .46 .46 .59 .87 .50 .88 .90 .53 .74 .64 .46 .44 .44 .00 .00 .00
.00 .00 .00 .38 .47 .39 .57 .91 .83 .87 .88 .88 .86 .56 .43 .37 .35 .37 .00 .00
.00 .00 .00 .37 .47 .41 .89 .82 .87 .93 .88 .91 .88 .88 .51 .49 .44 .37 .00 .00
.00 .00 .00 .00 .00 .00 .00 .00 .00 .00 .00 .00 .00 .00 .00 .00 .00 .00 .00 .00

Figure 6-4. Transmissivity Map of Synthetic Aquifer ($ft.^2/s$).

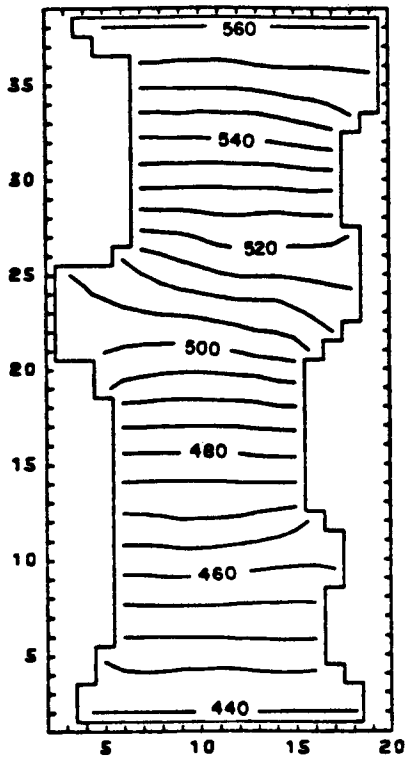

Figure 6-5. Hydraulic Head Contours of the Synthetic Aquifer at the End of the Fifth Year (ft.).

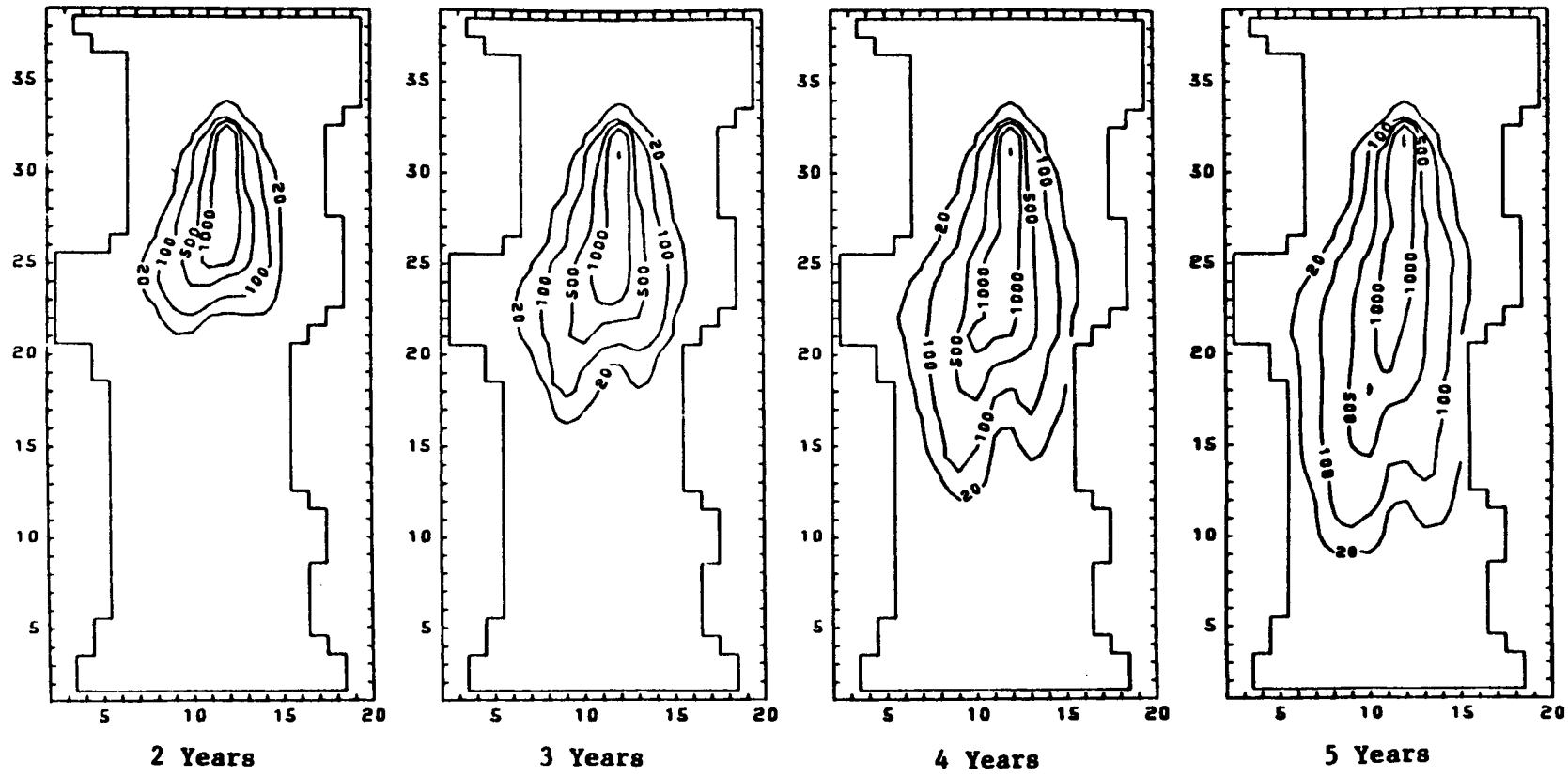

Figure 6-6. Concentration Contours of the Synthetic Aquifer at the End of the Second, Third, Fourth and Fifth Years.

Uncertainty Generation

To make the generated data more realistic, noise terms for heads and concentrations were produced from the block random field generator introduced in Chapter 5 and were added to the generated observations. The addition of the noise terms was also done in a manner that did not allow easy access to the data from the investigators.

To obtain the correlated error terms for the hydraulic heads, a serial correlation of .95 and a spatial correlation which decays with distance according to the modified Bessel function (Eq. (5.13)) were used. The decaying pattern of the Bessel function was set such that the correlation was 0.90 at one nodal distance (1000 feet). The error terms for the concentrations were a combination of both correlated and uncorrelated random fields. The correlated terms had a .90 serial correlation and spatial correlation according to the modified Bessel function. The decaying pattern was set with .80 correlation at one nodal distance (1000 feet). Both the correlated and the uncorrelated terms had mean zero and variance one. The two terms were added together to form a more realistic noise for concentration. The combination of a correlated and uncorrelated random field was used to represent the expected higher level of uncorrelated measurement errors for concentration.

The noise terms generated were five years in length. In sampling, the corresponding noise terms at the same node and time step were added to the observations, according to the following equations:

$$H'_o = H_o + \alpha_n \xi_h \tag{6.1}$$

$$C'_o = C_o + \alpha_c \xi_c \qquad (6.2)$$

where,

H'_o = observed head at a particular node and time step

H_o = computed head at a particular node and time step from the synthetic aquifer

ξ_h = random, correlated noise term for head, N(0,1)

α_n = standard deviation of noise

C'_o = observed concentration at a particular node and time step

C_o = computed concentration at a particular node and time step from the synthetic aquifer

ξ_c = random, correlated noise term for concentration, N(0,1)

$\alpha_c = (\alpha'_c)(C_o)$

α'_c = percentage of concentration for standard deviation

Three types of uncertainty were investigated in the study. Type I had no error and was introduced as a control for the experiments. The second type (Type II) had a standard deviation of one foot for head values, and 10 percent perturbation ($\alpha_c = 0.10$) for concentration values. The third type (Type III) had a standard deviation of five feet for the hydraulic heads and 25 percent perturbation ($\alpha_c = 0.25$) for concentrations. The three types of uncertainty are shown in Table 6.3. All types of uncertainty have the same fixed correlation structure introduced above.

Table 6-3. Uncertainty Levels in Data.

	Head (α_n)	Conc (α'_c)
Type I	0	0
Type II	1'	.10 (10 percent)
Type III	5'	.25 (25 percent)

Sampling Strategy Design

Six sampling strategies were designed to assess the data requirements for calibration of the USGS-MOC model. The strategies were also chosen to allow a brief evaluation of space/time tradeoffs in additional data for model calibration. The sampling strategies selected for this study are shown in Table 6-4.

The locations of the selected observation wells are shown in Figure 6-1 for the 12 well case, Figure 6-7 for the 18 well case, and Figure 6-8 for the eight well case. The locations were chosen to give a wide coverage of the aquifer and also to capture enough information about the contaminant plume.

To investigate the effects of parameterization on the aquifers, calibration attempts were made assuming that transmissivity in the aquifer could be represented by one, three, and six zones. The zoning patterns were determined from an estimated transmissivity map (to be discussed in Chapter 8).

For each of the cases in Tables 6-3 and 6-4, the parameter values which gave the best fit between the model solutions and the observations were determined by the PI-MOC algorithm introduced in Chapters 3 and 4. The identified parameters were then used in the model to predict the heads and contaminant

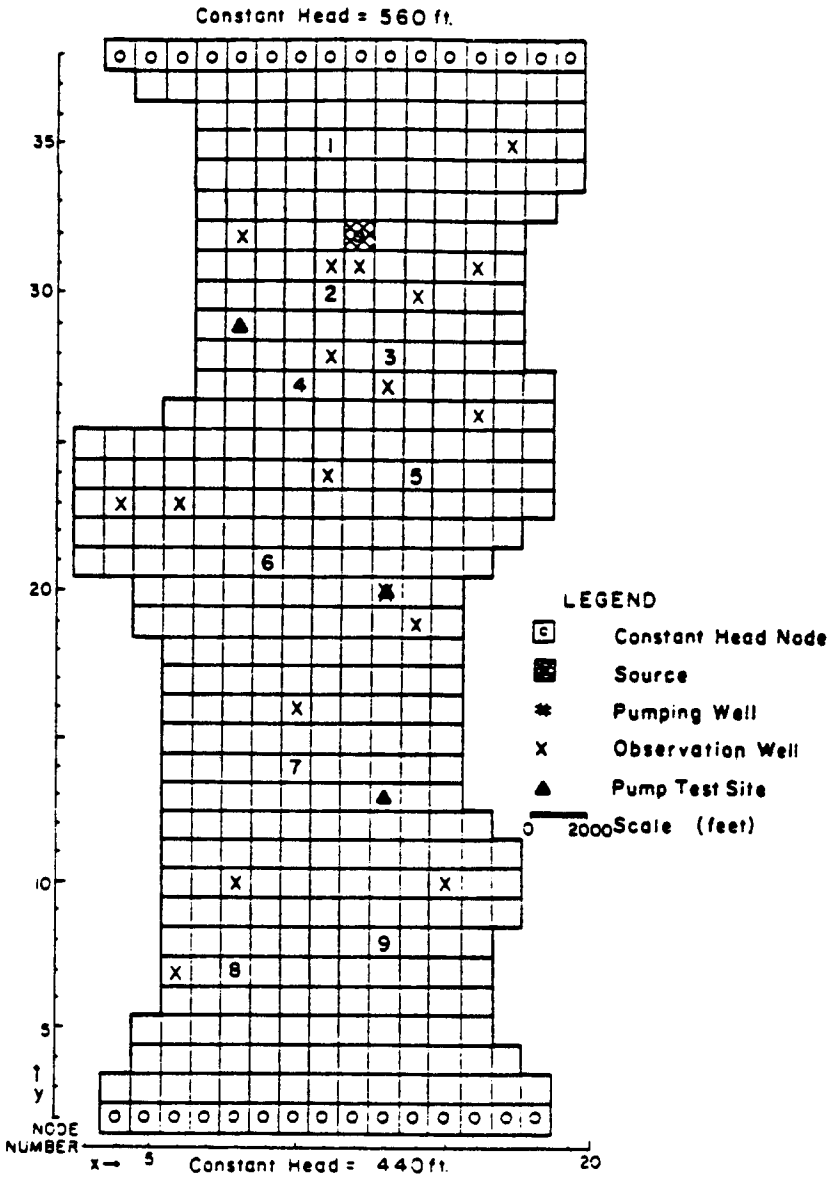

Figure 6-7. Synthetic Aquifer Configuration, Showing the Locations of 18 Observation Wells for Data Strategy D.

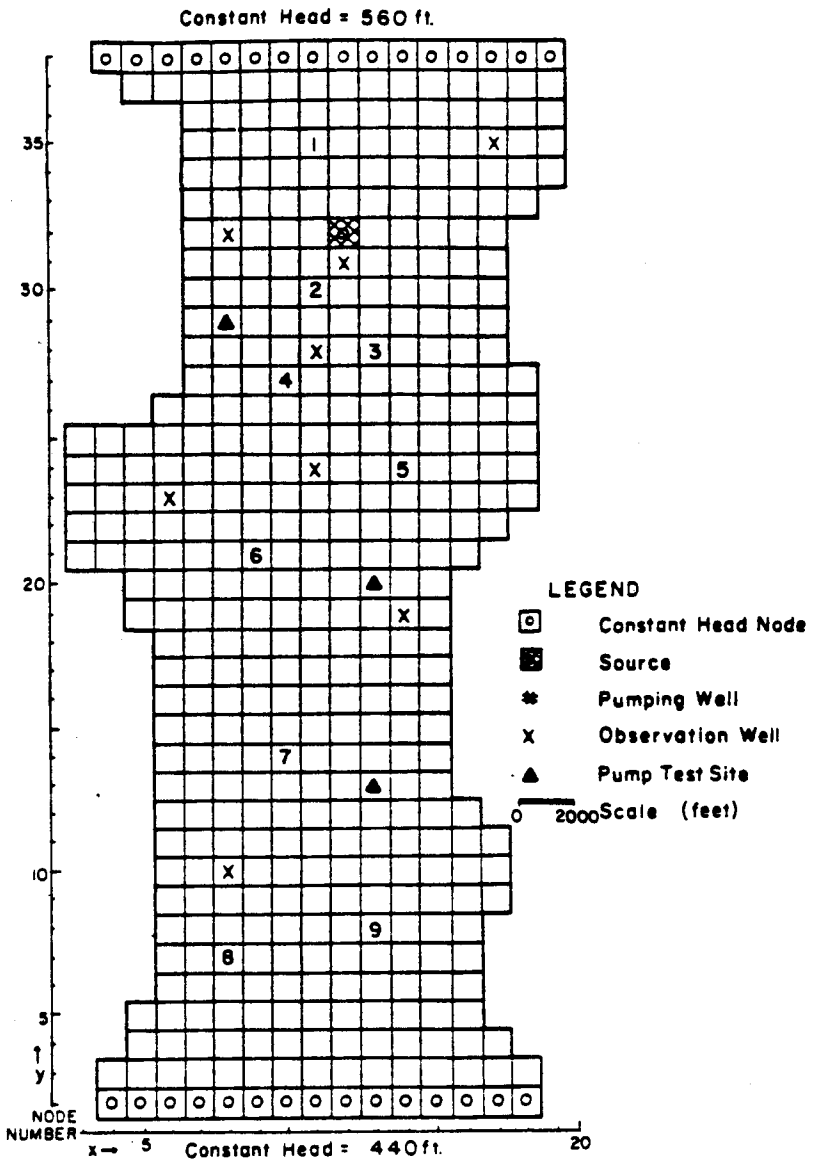

Figure 6-8. Synthetic Aquifer Configuration, Showing the Locations of 8 Observation Wells for Data Strategy E.

Table 6-4. Sampling Strategies Used for the Study.

Sampling Strategy	Number of Observation Wells	Number of Years of Monthly Observations
A	12	2 years of monthly head and concentration values
B	12	3 years of monthly head and concentration values
C	12	4 years of monthly head and concentration values
D	18	2 years of monthly head and concentration values
E	8	2 years of monthly head and concentration values
F	12	Using interpolated transmissivities (from the 12 point estimates in Table 6-2) and 2 years of monthly concentration data

plumes for each case. The predicted results were compared with the "actual data" (Figs. 6-5 and 6-6) obtained by using the "true parameters" (in Figs. 6-2, 6-3, and 6-4). The results are given in the next chapter.

CHAPTER 7

RESULTS AND DISCUSSION

To begin the parameter identification runs according to the designed procedure described at the end of the last chapter, aquifer thickness and initial water table at each grid point had to be estimated. Aquifer thicknesses were estimated using the 23 point estimates (Table 6-1) and a nearest neighbor interpolating scheme from the contouring package Surface II (Sampson, 1984). The interpolated results are shown in Figure 7-1. Initial heads, on the other hand, were linearly interpolated from the constant head boundary conditions. The interpolated values were found to agree well with the point estimates available from observation and pumping wells. In all the runs of PI-MOC (to be described later), it was found that the aquifer reached steady-state conditions within one or two months (time period used in USGS-MOC simulations), and therefore an accurate estimate of initial hydraulic head conditions was not important. A similar observation was also reported by Gates and Kiesel (1974) in their study of the worth of additional data to the calibration effort.

The next important information needed for running the experiments was the transmissivity zoning patterns. Using the 12 point estimates of transmissivity in Table 6-1, transmissivities at all the grid points were estimated by the Surface II contouring package (Sampson, 1984). The interpolated values are shown in Figure 7-2. From the generated contour map, zones of constant transmissivity were drawn for the planned three and six zone

0. 0. 0. 0. 0. 0. 0. 0. 0. 0. 0. 0. 0. 0. 0. 0. 0. 0. 0. 0.
0. 0. 0.104.106.108.109.110.111.111.110.109.105. 99. 92. 88. 86. 85. 85. 0.
0. 0. 0. 0.105.107.109.110.111.111.111.110.107. 99. 91. 86. 84. 84. 84. 0.
0. 0. 0. 0. 0. 0.108.110.111.112.112.111.108. 99. 89. 84. 82. 83. 83. 0.
0. 0. 0. 0. 0. 0.106.109.111.112.112.112.109.100. 89. 83. 82. 82. 83. 0.
0. 0. 0. 0. 0. 0.102.107.110.112.112.112.110.103. 92. 84. 83. 83. 84. 0.
0. 0. 0. 0. 0. 0. 95.100.106.110.111.112.111.108.101. 91. 86. 85. 0. 0.
0. 0. 0. 0. 0. 0. 85. 91.100.108.111.112.112.112.110.103. 95. 0. 0. 0.
0. 0. 0. 0. 0. 0. 78. 81. 93.106.110.113.113.114.113.110.104. 0. 0. 0.
0. 0. 0. 0. 0. 0. 73. 72. 84.105.106.110.113.114.113.111.105. 0. 0. 0.
0. 0. 0. 0. 0. 0. 70. 68. 79.105.110.111.113.113.112.105. 97. 0. 0. 0.
0. 0. 0. 0. 0. 0. 73. 75. 95.111.114.113.113.112.103. 91. 87. 0. 0. 0.
0. 0. 0. 0. 0. 0. 82. 93.109.113.113.113.113.107. 86. 78. 78. 81. 0. 0.
0. 0. 0. 0. 0. 72. 83. 99.110.113.113.112.109. 99. 81. 75. 77. 79. 0. 0.
0. 0. 63. 61. 60. 62. 71. 91.109.113.113.112.108.105. 92. 79. 79. 81. 0. 0.
0. 0. 61. 58. 55. 54. 60. 81.105.113.113.112.108.108.105. 92. 86. 86. 0. 0.
0. 0. 59. 56. 54. 52. 57. 81.104.111.113.112.109.108.106.101. 95. 93. 0. 0.
0. 0. 60. 58. 56. 55. 67. 98.108.110.111.112.111.110.108.105.102. 0. 0. 0.
0. 0. 63. 62. 62. 68. 87.107.110.110.111.113.113.112.110.109. 0. 0. 0. 0.
0. 0. 0. 0. 73. 81. 96.107.110.110.112.113.114.111.110. 0. 0. 0. 0. 0.
0. 0. 0. 0. 85. 92.101.107.110.111.112.113.112.109.110. 0. 0. 0. 0. 0.
0. 0. 0. 0. 0.101.107.111.113.114.113.112.111.110.110. 0. 0. 0. 0. 0.
0. 0. 0. 0. 0.108.112.113.114.115.114.112.110.109.109. 0. 0. 0. 0. 0.
0. 0. 0. 0. 0.111.113.114.114.115.114.111.107.106.105. 0. 0. 0. 0. 0.
0. 0. 0. 0. 0.112.112.112.113.113.112.107.101. 99. 99. 0. 0. 0. 0. 0.
0. 0. 0. 0. 0.111.111.111.111.111.110.100. 95. 95. 94. 0. 0. 0. 0. 0.
0. 0. 0. 0. 0.110.110.110.110.110.106. 96. 94. 94. 90. 0. 0. 0. 0. 0.
0. 0. 0. 0. 0.109.109.109.109.107.102. 96. 93. 90. 84. 80. 0. 0. 0. 0.
0. 0. 0. 0. 0.108.109.109.108.105.100. 94. 88. 80. 75. 76. 78. 0. 0. 0.
0. 0. 0. 0. 0.107.109.110.109.104. 98. 92. 87. 77. 73. 74. 76. 0. 0. 0.
0. 0. 0. 0. 0.105.106.107.106.102. 97. 93. 92. 84. 76. 76. 78. 0. 0. 0.
0. 0. 0. 0. 0.102.100. 99.100. 99. 96. 94. 94. 91. 84. 81. 0. 0. 0. 0.
0. 0. 0. 0. 0. 99. 98. 97. 98. 98. 96. 94. 93. 92. 88. 85. 0. 0. 0. 0.
0. 0. 0. 0. 0. 99. 98. 97. 98. 97. 96. 94. 93. 92. 89. 87. 0. 0. 0. 0.
0. 0. 0. 0. 99. 99. 98. 98. 98. 97. 96. 94. 93. 92. 90. 88. 0. 0. 0. 0.
0. 0. 0. 0. 99. 99. 98. 98. 97. 97. 96. 94. 93. 92. 91. 89. 88. 0. 0. 0.
0. 0. 0. 99. 99. 99. 98. 98. 97. 97. 96. 95. 93. 92. 91. 90. 89. 88. 0. 0.
0. 0. 0. 99. 99. 99. 98. 98. 97. 97. 96. 95. 94. 93. 92. 91. 90. 89. 0. 0.
0. 0. 0. 0. 0. 0. 0. 0. 0. 0. 0. 0. 0. 0. 0. 0. 0. 0. 0. 0.

Figure 7-1. Interpolated Aquifer Thicknesses Used in PI-MOC Calibration Runs (ft.).

.00 .00 .00 .00 .00 .00 .00 .00 .00 .00 .00 .00 .00 .00 .00 .00 .00 .00 .00 .00 .00
.00 .00 .00 .76 .77 .78 .78 .79 .80 .80 .80 .80 .81 .81 .81 .82 .82 .83 .83 .00
.00 .00 .00 .00 .76 .77 .78 .79 .80 .80 .80 .80 .81 .81 .82 .82 .83 .83 .84 .00
.00 .00 .00 .00 .00 .00 .77 .79 .80 .80 .80 .80 .81 .81 .82 .83 .83 .84 .84 .00
.00 .00 .00 .00 .00 .00 .76 .78 .79 .80 .80 .80 .81 .82 .83 .84 .84 .85 .85 .00
.00 .00 .00 .00 .00 .00 .74 .77 .79 .80 .80 .81 .82 .83 .84 .85 .86 .86 .86 .00
.00 .00 .00 .00 .00 .00 .70 .74 .77 .80 .82 .83 .84 .85 .86 .87 .87 .87 .00 .00
.00 .00 .00 .00 .00 .00 .64 .68 .75 .81 .85 .86 .87 .88 .89 .89 .89 .00 .00 .00
.00 .00 .00 .00 .00 .00 .56 .59 .70 .84 .88 .89 .90 .91 .91 .91 .90 .00 .00 .00
.00 .00 .00 .00 .00 .00 .48 .47 .61 .85 .90 .90 .93 .94 .94 .93 .91 .00 .00 .00
.00 .00 .00 .00 .00 .00 .44 .40 .54 .82 .90 .94 .98 .98 .96 .94 .92 .00 .00 .00
.00 .00 .00 .00 .00 .00 .50 .50 .72 .92 .94 .981.00 .99 .96 .93 .91 .00 .00 .00
.00 .00 .00 .00 .00 .00 .62 .72 .921.00 .97 .97 .98 .96 .92 .89 .87 .86 .00 .00
.00 .00 .00 .00 .00 .69 .73 .82 .93 .97 .95 .92 .89 .86 .83 .83 .82 .81 .00 .00
.00 .00 .71 .72 .73 .75 .79 .84 .88 .91 .89 .84 .79 .76 .77 .77 .78 .77 .00 .00
.00 .00 .74 .75 .77 .79 .81 .83 .84 .84 .81 .77 .75 .75 .75 .74 .74 .74 .00 .00
.00 .00 .77 .79 .80 .82 .83 .83 .83 .80 .74 .70 .71 .73 .72 .71 .70 .69 .00 .00
.00 .00 .80 .81 .82 .83 .84 .84 .84 .81 .69 .55 .53 .58 .61 .62 .63 .00 .00 .00
.00 .00 .81 .82 .82 .83 .83 .84 .85 .82 .63 .40 .34 .38 .46 .52 .00 .00 .00 .00
.00 .00 .00 .00 .82 .83 .83 .84 .84 .78 .56 .35 .30 .33 .39 .00 .00 .00 .00 .00
.00 .00 .00 .00 .83 .83 .82 .82 .80 .72 .54 .38 .33 .35 .40 .00 .00 .00 .00 .00
.00 .00 .00 .00 .00 .85 .84 .82 .80 .73 .61 .49 .42 .42 .46 .00 .00 .00 .00 .00
.00 .00 .00 .00 .00 .88 .88 .88 .87 .84 .78 .70 .64 .62 .62 .00 .00 .00 .00 .00
.00 .00 .00 .00 .00 .91 .93 .94 .95 .95 .92 .88 .85 .82 .80 .00 .00 .00 .00 .00
.00 .00 .00 .00 .00 .93 .95 .97 .98 .99 .98 .96 .95 .94 .91 .00 .00 .00 .00 .00
.00 .00 .00 .00 .00 .93 .95 .98 .991.00 .99 .99 .99 .98 .96 .00 .00 .00 .00 .00
.00 .00 .00 .00 .00 .92 .94 .97 .99 .99 .99 .991.00 .99 .97 .00 .00 .00 .00 .00
.00 .00 .00 .00 .00 .89 .91 .94 .96 .97 .97 .98 .99 .98 .97 .95 .00 .00 .00 .00
.00 .00 .00 .00 .00 .84 .86 .88 .91 .93 .94 .95 .96 .96 .95 .93 .92 .00 .00 .00
.00 .00 .00 .00 .00 .80 .80 .81 .84 .88 .90 .91 .92 .92 .92 .92 .92 .00 .00 .00
.00 .00 .00 .00 .00 .76 .75 .75 .78 .83 .88 .90 .90 .90 .91 .91 .91 .00 .00 .00
.00 .00 .00 .00 .00 .73 .72 .71 .73 .79 .86 .89 .90 .90 .90 .90 .00 .00 .00 .00
.00 .00 .00 .00 .00 .72 .71 .70 .71 .77 .84 .89 .90 .90 .90 .90 .00 .00 .00 .00
.00 .00 .00 .00 .00 .72 .71 .71 .72 .76 .83 .87 .89 .89 .89 .89 .00 .00 .00 .00
.00 .00 .00 .00 .74 .73 .72 .72 .74 .77 .82 .85 .87 .88 .88 .88 .00 .00 .00 .00
.00 .00 .00 .00 .75 .74 .74 .74 .76 .78 .81 .84 .86 .87 .87 .88 .88 .00 .00 .00
.00 .00 .00 .76 .76 .75 .75 .76 .77 .79 .81 .83 .85 .86 .87 .87 .87 .87 .00 .00
.00 .00 .00 .77 .77 .76 .77 .77 .78 .80 .81 .83 .84 .85 .86 .86 .87 .87 .00 .00
.00 .00 .00 .00 .00 .00 .00 .00 .00 .00 .00 .00 .00 .00 .00 .00 .00 .00 .00 .00 .00

Figure 7-2. Interpolated Transmissivity Field Used for Delineating Transmissivity Zoning Patterns and for Data Strategy F ($ft.^2/s$).

cases described earlier. The shapes of the three and six zone transmissivity zones are shown in Figures 7-3 and 7-4, respectively.

Once the above parameters and zone shapes were determined, the PI-MOC was run for each of the selected combinations of sampling strategies, zoning patterns, and data uncertainty levels. The identified transmissivities and dispersivities for all the sampling stategies with uncertainty levels I, II and III are shown in Tables 7-1, 7-2, and 7-3. A total of over 250 runs of PI-MOC were completed for the selected combinations.

For most calibration runs with higher data uncertainty levels, transmissivity upper and/or lower bounds had to be adjusted to insure that parameter values were found which did not deviate radically from the interpolated transmissivity map (Fig. 7-2). Bounds were also used at times to keep the PI-MOC algorithm stable. For Type III uncertainty level, for example, the PI algorithm was unable to find transmissivity values for the six zone case with any sampling strategy. These results suggest that when data are highly uncertain, the number of zones must be reduced. Sampling strategy E (8 wells, 2 years) did not contain sufficient data to calibrate for six zones of transmissivities and dispersivities. In fact, obtaining parameter estimates with data from sampling strategy E was difficult for nearly all cases.

The estimated parameters (Tables 7-1, 7-2, and 7-3) were used to predict five years of hydraulic heads and concentrations at each computational node, and were compared with the actual hydraulic heads and concentrations (shown in Figs. 6-5 and 6-6), which were made available to the investigator after all the PI-MOC runs were completed. The comparison analysis was accomplished both

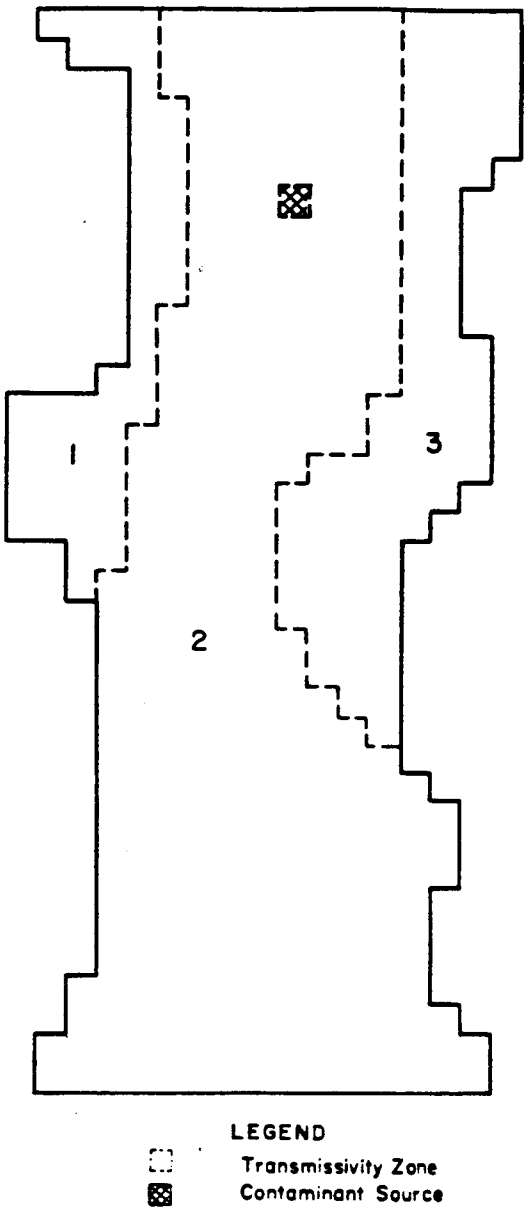

Figure 7-3. Three Zone Transmissivity Characterization Used in PI-MOC Calibration Runs.

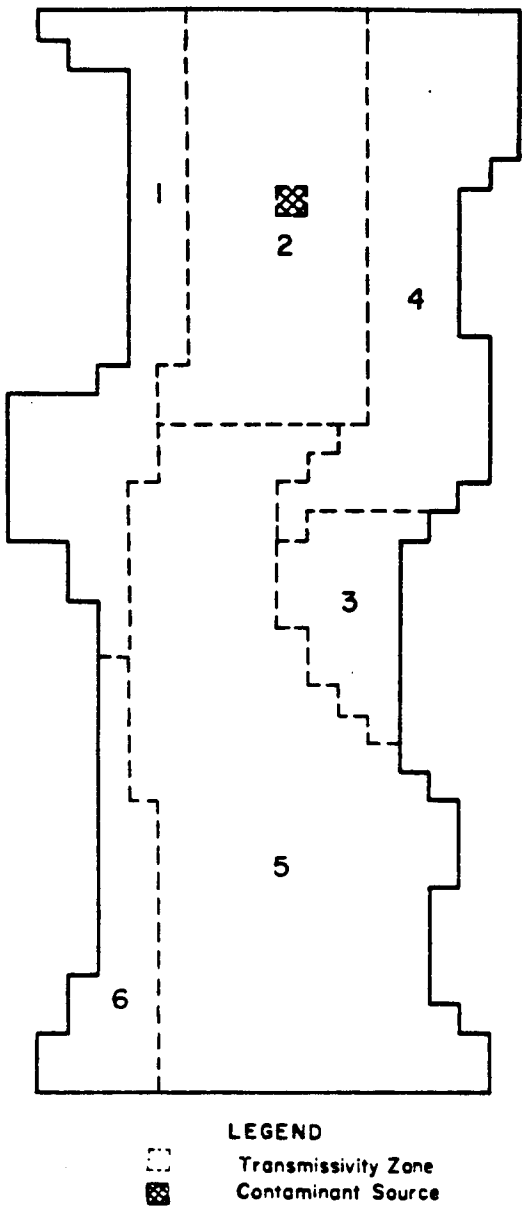

Figure 7-4. Six Zone Transmissivity Characterization Used in PI-MOC Calibration Runs.

Table 7-1. Parameters Identified by PI-MOC with Uncertainty Type I Data and the Listed Transmissivity Characterizations and Sampling Strategies.

Number of Transmissivity Zones		Sampling Strategy	Transmissivity ($Ft.^2/s$) in Zone Number (Refer to Figures 7-1 and 7-2) 1	2	3	4	5	6	Dispersivities α_L	α_T
6	A	12 w, 2 yr	.5535	.8251	.5165	.5008	.7397	.7137	126.4	82.0
6	B	12 w, 3 yr	.5535	.8251	.5166	.5008	.7397	.7137	136.2	79.3
6	C	12 w, 4 yr	.5535	.8251	.5166	.5008	.7397	.7137	137.1	88.7
6	D	18 w, 2 yr	.4836	.8211	.5200	.4498	.6939	.6828	138.9	94.1
6	E	8 w, 2 yr	.6301	.8300	.5016	.6325	.7650	.9000	———	——*
3	A	12 w, 2 yr	.7201	.7835	.5170				174.7	84.3
3	B	12 w, 3 yr	.7205	.7815	.5155				163.5	82.0
3	D	12 w, 2 yr	.7255	.8249	.5367				115.4	89.8
3	E	8 w, 2 yr	.7823	.8300	.5457				109.3	25.7
1	A	12 w, 2 yr	.5508						627.0	115.3
1	B	12 w, 3 yr	.5471						617.2	101.6
1	C	18 w, 2 yr	.5511						657.9	132.9
1	D	8 w, 2 yr	.6075						———	———*
Interpolated Transmissivities									174.5	99.9

* PI-MOC unable to identify parameters

Table 7-2. Parameters Identified by PI-MOC with Uncertainty Type II Data and the Listed Transmissivity Characterizations and Sampling Strategies.

Number of Transmissivity Zones		Sampling Strategy	Transmissivity ($Ft.^2/s$) in Zone Number (Refer to Figures 7-1 and 7-2) 1	2	3	4	5	6	Dispersivity α_L	α_T
6	A	12 w, 2 yr	.6256	.7655	.4874	.6098	.7163	.9000	241.0	93.5
6	B	12 w, 3 yr	.7229	.8154	.6289	.6956	.8261	.9000	97.6	75.5
6	C	12 w, 4 yr	.5753	.7923	.6000	.6578	.7352	.8064	126.5	84.3
6	D	18 w, 2 yr	.5778	.8280	.5490	.6145	.7560	.9000	125.5	95.8
6	E	8 w, 2 yr	———	———	———	———	———	———	———	———*
3	A	12 w, 2 yr	.7784	.7979	.5050				176.9	89.8
3	B	12 w, 3 yr	.7540	.8222	.5400				110.9	77.7
3	C	12 w, 4 yr	.7998	.8300	.5323				113.1	91.7
3	D	18 w, 2 yr	.7623	.7992	.5102				166.8	99.5
3	E	8 w, 2 yr	.7951	.8151	.5800				148.8	29.5
1	A	12 w, 2 yr	.5703						532.7	109.2
1	B	12 w, 3 yr	.5695						537.5	101.1
1	C	18 w, 2 yr	.5648						578.5	131.9
1	D	8 w, 2 yr	.6347						———	———*
Interpolated Transmissivities									165.0	104.4

* PI-MOC unable to identify parameters

Table 7-3. Parameters Identified by PI-MOC with Uncertainty Type III Data and the Listed Transmissivity Characterizations and Sampling Strategies.

Number of Transmissivity Zones	Sampling Strategy	Transmissivity ($Ft.^2/s$) in Zone Number (Refer to Figures 7-1 and 7-2)			Dispersivities	
		1	2	3	α_L	α_T
3	A 12 w, 2 yr	.8500	.8315	.5194	114.8	87.7
3	B 12 w, 3 yr	.8500	.8322	.5400	115.9	83.0
3	C 12 w, 4 yr	.8500	.8207	.5300	136.1	93.2
3	D 18 w, 2 yr	.8500	.7113	.4420	293.1	120.8
3	E 8 w, 2 yr	.8500	.7501	.6800	———	———*
1	A 12 w, 2 yr	.6685			322.2	103.5
1	B 12 w, 3 yr	.6628			350.0	95.7
1	D 18 w, 2 yr	.6276			413.0	125.0
1	E 8 w, 2 yr	.7732			———	———*
Interpolated Transmissivities					141.8	109.4

* PI-MOC unable identify parameters

in graphical form, using the Surface II contouring package (Sampson, 1984), and by a sum of squares analysis. The sum of squares analysis for the hydraulic heads, concentrations, and the logarithm of concentration are presented in Tables 7-4, 7-5, and 7-6 for uncertainty Types I, II, and III, respectively.

Generally, for all the predictive simulations, the PI-MOC procedure was able to find parameters which would preserve the plume shape well. The actual concentration magnitudes, especially for higher concentrations (1000 units and above), were underpredicted. The preservation of plume shape was the result of using logarithms as a weighting function in the parameter identification formulation. However, the weighting function did not tend to find dispersivities that preserved large concentration magnitudes as well. In formulation of the USGS-MOC model, advection was assumed to be the dominant contaminant transport mechanism. If the weighting function had not been used, PI-MOC would have found much higher dispersivities (as was observed in preliminary testing of PI-MOC), possibly violating the advection dominant transport assumption. A brief analysis of the experiments with different transmissivity zoning patterns is given in the next section.

Effects of Transmissivity Zoning

None of the homogeneous (transmissivity assumed to be constant throughout the aquifer) cases seemed to give satisfactory results in the sum of squares analysis of concentration for any of the three data uncertainty cases tested. The plume shapes for the homogeneous cases were generally shortened in the longitudinal direction. The dispersivities identified for these runs were

Table 7-4. Sum of Squares Analysis; Comparing Monthly Predicted Hydraulic Heads and Concentrations Throughout the Domain of the Aquifer Versus the Actual Values from the Synthetic Aquifer for a Five Year Simulation. Uncertainty Type I Data, and the Listed Transmissivity Characterizations and Data Strategies Were Used to Estimate the Parameters.

Number of Transmissivity Zones	Sampling Strategy	$\Sigma(H_r-H_e)^2$	$\Sigma(C_r-C_e)^2$ ($\times 10^6$)	$\Sigma(\ln C_r-\ln C_e)^2$
6	A 12 w, 2 yr	9,549	216	3537
6	B 12 w, 3 yr	9,549	214	3682
6	C 12 w, 4 yr	9,549	227	3486
6	D 12 w, 4 yr	8,726	251	3181
6	E 8 w, 2 yr	———	——	——*
3	A 12 w, 2 yr	11,653	257	4635
3	B 12 w, 3 yr	11,670	256	4665
3	D 18 w, 2 yr	11,797	277	4625
3	E 8 w, 2 yr	13,184	322	16,385
1	A 12 w, 2 yr	25,409	413	12,301
1	B 12 w, 3 yr	25,173	397	12,575
1	D 18 w, 2 yr	25,428	447	12,912
1	E 8 w, 2 yr	———	——	———*
Using Interpolated Transmissivities		61,014	985	10,841

* PI-MOC Unable to Identify Parameters

Table 7-5. Sum of Squares Analysis; Comparing Monthly Predicted Hydraulic Heads and Concentrations Throughout the Domain of the Aquifer Versus the Actual Values from the Synthetic Aquifer for a Five Year Simulation. Uncertainty Type II Data, and the Listed Transmissivity Characterizations and Data Strategies Were Used to Estimate the Parameters.

Number of Transmissivity Zones	Sampling Strategy	$\Sigma(H_r-H_e)^2$	$\Sigma(C_r-C_e)^2$ ($\times 10^6$)	$\Sigma(\ln C_r-\ln C_e)^2$
6	A 12 w, 2 yr	13,388	367	4,792
6	B 12 w, 3 yr	10,287	197	4,596
6	C 12 w, 2 yr	9,593	183	3,933
6	D 18 w, 2 yr	10,542	308	3,940
6	E 8 w, 2 yr	———	—	———*
3	A 12 w, 2 yr	13,236	312	4,878
3	B 12 w, 3 yr	12,232	291	4,824
3	C 12 w, 4 yr	13,872	340	4,780
3	D 18 w, 2 yr	12,771	317	4,782
3	E 8 w, 2 yr	15,888	283	15,030
1	A 12 w, 2 yr	26,988	388	10,703
1	B 12 w, 3 yr	26,982	375	10,794
1	D 18 w, 2 yr	26,494	434	11,679
1	E 8 w, 2 yr	———	—	———*
Using Interpolated Transmissivities		61,014	991	10,548

* PI-MOC Unable to Identify Parameters

Table 7-6. Sum of Squares Analysis; Comparing Monthly Predicted Hydraulic Heads and Concentrations Throughout the Domain of the Aquifer Versus the Actual Values from the Synthetic Aquifer for a Five Year Simulation. Uncertainty Type III Data, and the Listed Transmissivity Characterizations and Data Strategies Were Used to Estimate the Parameters.

Number of Transmissivity Zones	Sampling Strategy	$\Sigma(H_r-H_e)^2$	$\Sigma(C_r-C_e)^2$ ($\times 10^6$)	$\Sigma(\ln C_r-\ln C_e)^2$
6	—	—	—	—*
3	A 12 w, 2 yr	16,401	371	4,880
3	B 12 w, 3 yr	16,882	370	5,167
3	C 12 w, 4 yr	16971	399	2,941
3	D 18 w, 2 yr	18,457	494	6,585
3	E 8 w, 2 yr	———	—	—*
1	A 12 w, 2 yr	40,378	405	6,466
1	B 12 w, 3 yr	39,455	392	6,944
1	C 12 w, 4 yr	———	—	—*
1	D 18 w, 2 yr	34,010	427	7,869
1	E 8 w, 2 yr	———	—	—*
Using Interpolated Transmissivities		61,014	949	10,191

* PI-MOC Unable to Determine Values

always very high (400 to 600 feet for longitudinal dispersivity), which implies that the PI-MOC tended to determine values which were forcing dispersion to be more dominant. The sum of squares analysis showed that even the head predictions were poor when the aquifer was assumed to be homogeneous. Treating this aquifer as homogeneous with respect to transmissivity was not a good modeling approach and resulted in significant prediction errors.

The three zone case preserved the length of the contaminant plume better than the homogeneous case. The sum of squares analysis also showed that treating the aquifer as having three transmissivity zones significantly improved the predicted results for data uncertainty Types I and II. With Type III uncertainty level, the sum of squares concentration analysis for the homogeneous case and the three zone case were about even. Using three transmissivity zones, piezometric head predictions were greatly improved (over the homogeneous case) for all uncertainty levels.

Among all the cases investigated, the six zone case gave the best results, both in preserving plume shape and in predicting concentration magnitudes. Transmissivity values, however, could be successfully determined only from data with Type I and II uncertainty. This suggests that as the uncertainty in data increases, the number of zones for transmissivity must be reduced to obtain acceptable results. Calibrations with Type II uncertainty were also difficult, as careful selection of upper and lower transmissivity bounds had to be established in order to obtain acceptable results. Once transmissivities were found, dispersivity values were determined quickly by PI-MOC, except for the most limited data case, E (eight wells, two years). Figure 7-5 shows the predicted concentrations at the end of the second,

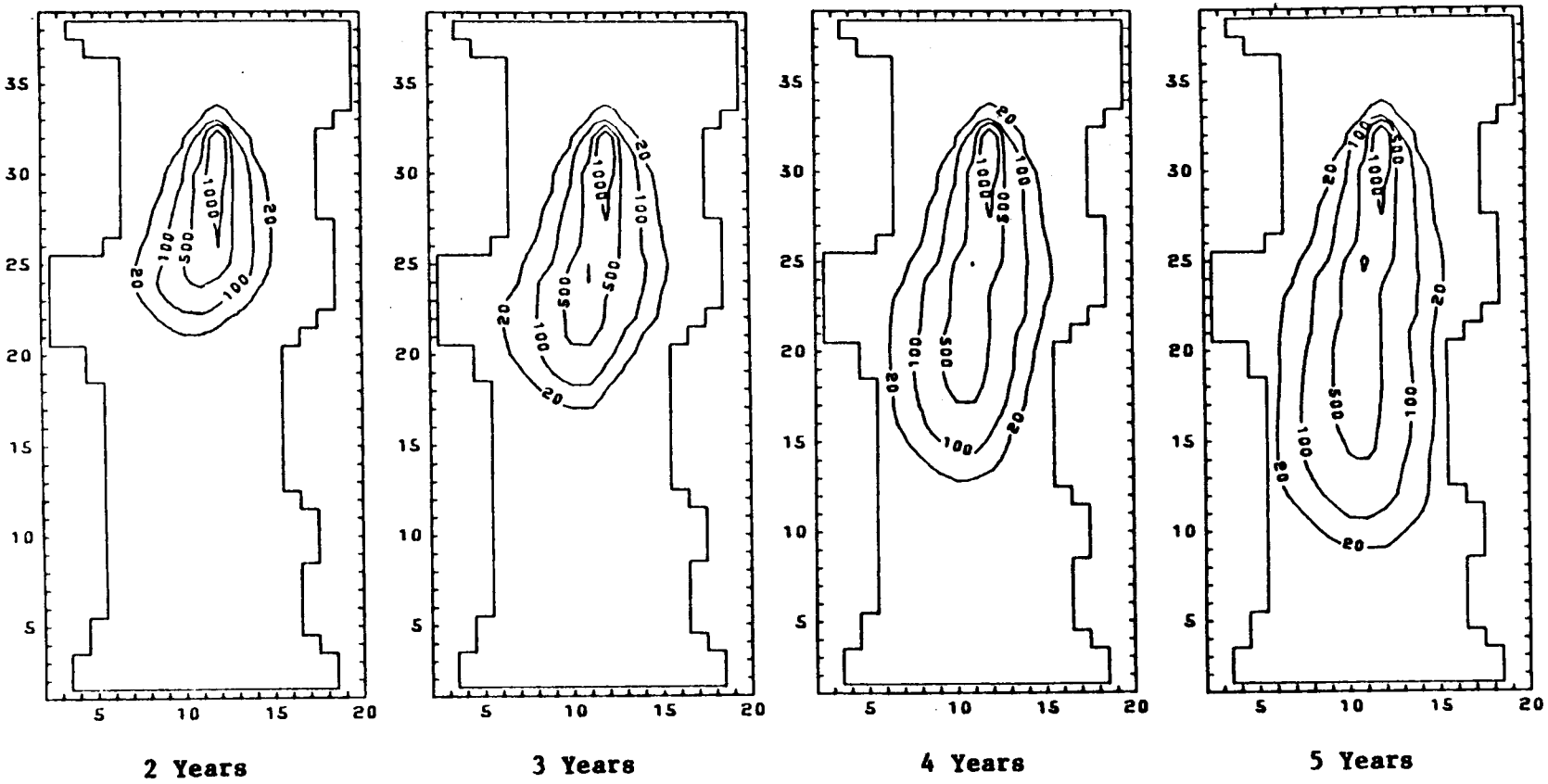

Figure 7-5. Predicted Concentration Contours at the End of the Second, Third, Fourth, and Fifth Years, Using Parameters Determined by PI-MOC with Data Strategy A (12 Wells, 2 Years), Six Zone Transmissivity Characterization, and Data Uncertainty Type I.

fourth, and the fifth year, using parameters determined from strategy A (12 wells, two years), for six transmissivity zones, and Type I uncertainty. By comparing these with the actual concentration plots (Fig. 6-5), it is apparent that general plume shapes were again well preserved, but the high concentrations (1000 units and above) were underpredicted in the latter years of the five-year simulations.

To compare the effect of increased parameterization of transmissivities on concentration predictions, the five-year prediction of concentrations using parameters estimated with Type II uncertainty and sampling strategies A and B are shown in Figures 7-6 and 7-7, respectively. A comparison with the actual concentrations (Fig. 6-6) shows that as parameterization improves, so does the contaminant plume prediction. The sum of squares analysis (Tables 7-4, 7-5, and 7-6) also shows that improved parameterization of transmissivity again improved parameter estimates.

Results Using Interpolated Transmissivities

In many actual applications, the transmissivity data for the model are estimated using point estimates from well logs or pump tests. In order to assess the effectiveness of using such interpolated transmissivity field data in contaminant transport prediction, the following experiment was conducted.

Using the 12 point estimates of transmissivities (Table 6-1), an interpolated field of transmissivities was first generated using the Surface II contouring package (Sampson, 1984). With interpolated transmissivity values, the PI-MOC algorithm was then used to identify only dispersivities

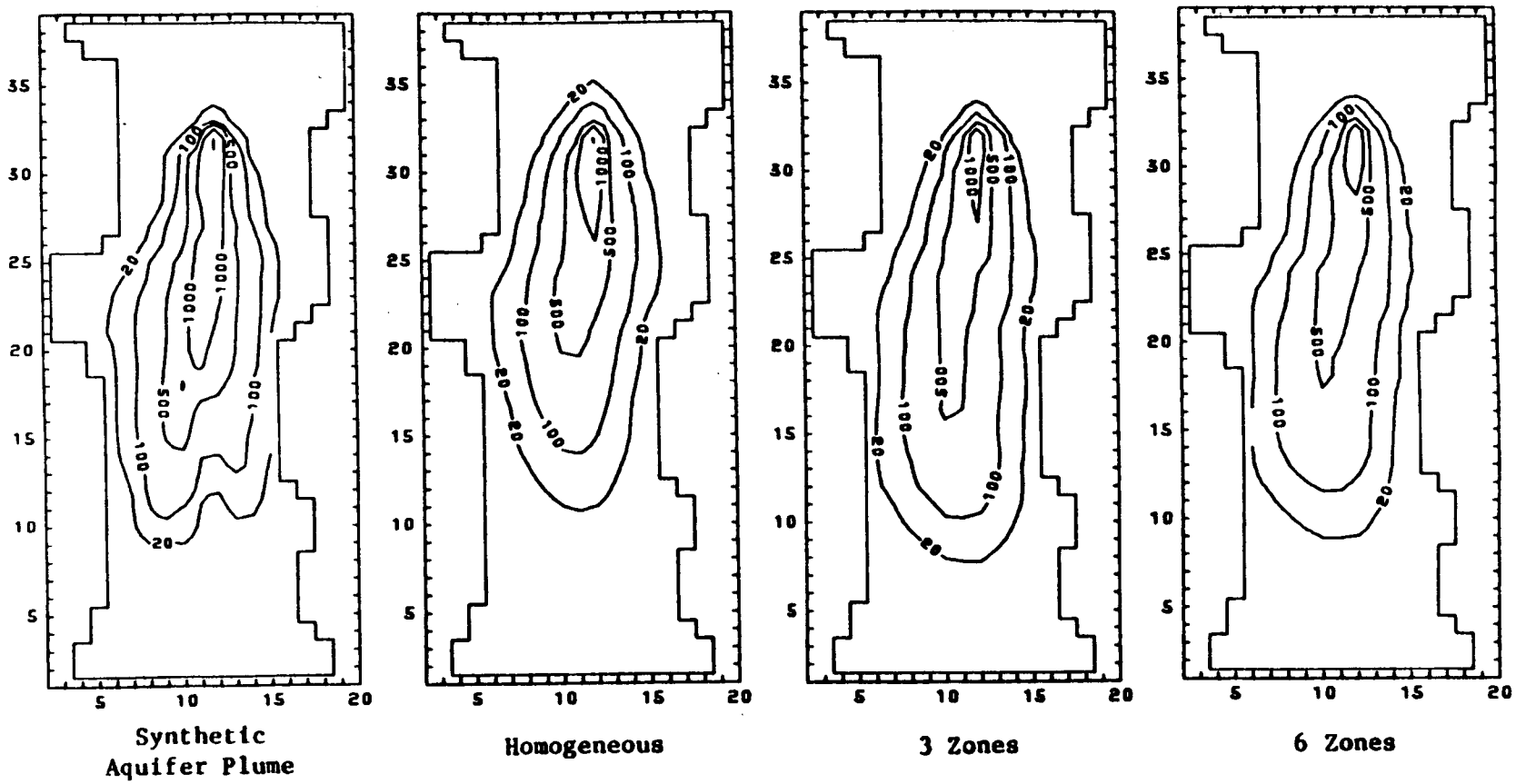

Figure 7-6. Comparison of Transmissivity Characterizations. Concentration Contour Predictions at the End of the Fifth Year, Using PI-MOC Determined Parameters, with Data Strategy A (12 Wells, 2 Years) and Type II Data Uncertainty.

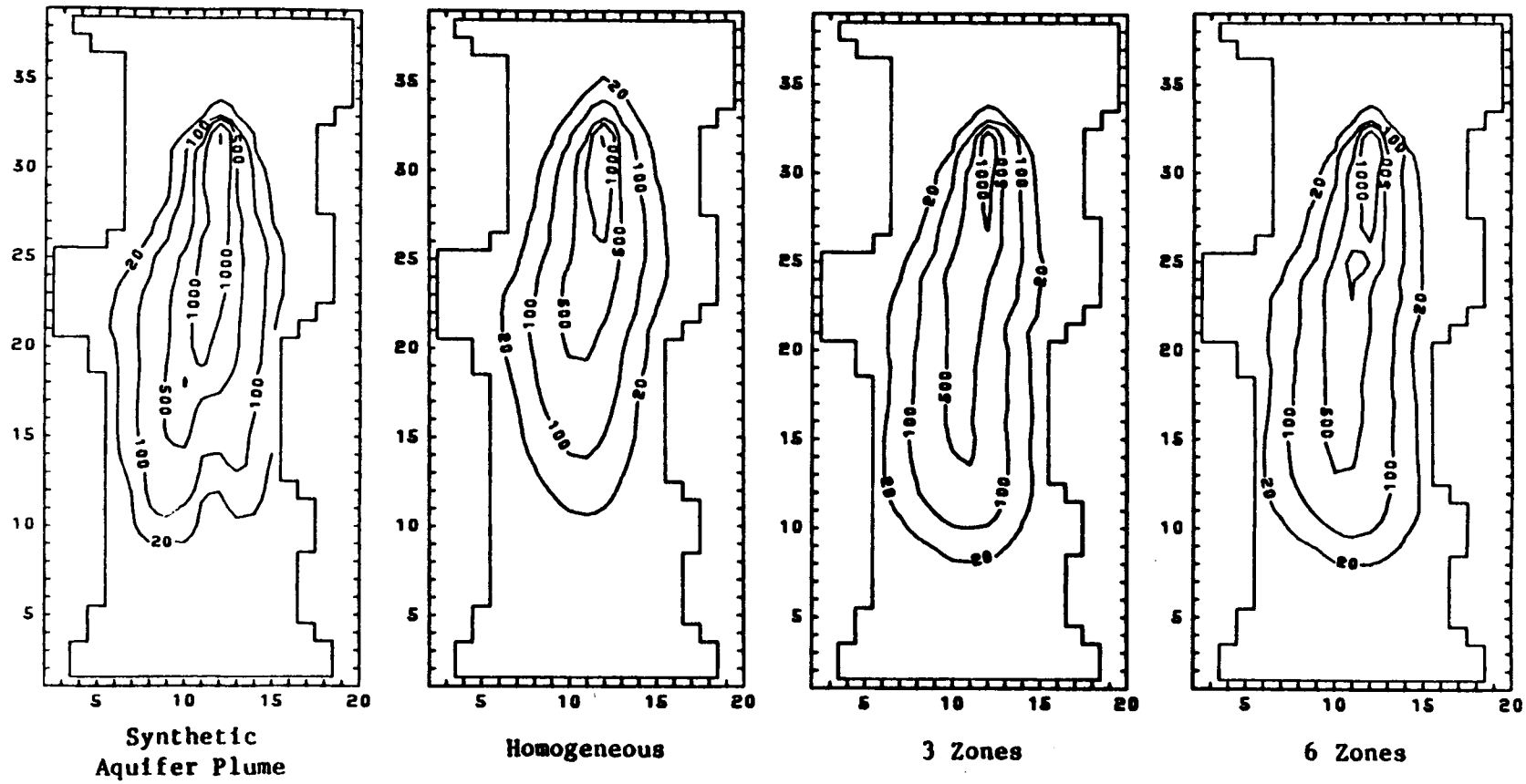

Figure 7-7. Comparison of Transmissivity Characterizations. Concentration Contour Predictions at the End of the Fifth Year, Using PI-MOC Determined Parameters, with Data Strategy B (12 Wells, 3 Years) and Type II Data Uncertainty.

with data from strategy A (12 wells, 2 years) for uncertainty Types I, II, and III.

The predictions made from the parameters determined by this method are given in Tables 7-4, 7-5, and 7-6. As can be seen in the tables, the predictions based on the interpolated transmissivities and the PI-determined dispersivities did a poor job of estimating concentration magnitudes. The predictions of the concentration plume and the head contours at the end of a five-year simulation are shown in Figure 7-8. The overall plume shape was correct for low concentrations, but the higher values were grossly underestimated. In comparing the predicted head contours with the actual ones in Figure 6-5, however, one can see that the two do not deviate significantly from each other. The sum of squares analysis (Tables 7-4, 7-5, and 7-6) indicated that this approach was the worst method for predicting heads for the aquifer. The results of this experiment clearly show that the proposed PI method is quite an attractive tool for model calibration. Even in the cases where the aquifer was assumed as homogeneous, PI-MOC was able to determine parameter values which were far more accurate than the interpolated estimates.

Comparison of Sampling Strategies

As expected, the most limiting case (Case E, eight wells, two years) was by far the worst sampling strategy in terms of predictive capability. The PI-MOC algorithm had problems identifying not only transmissivities, but also dispersivities. This was the only strategy where the PI-MOC algorithm had difficulty identifying dispersivities. Using data from sampling strategy E, Type I uncertainty, and three transmissivity zones, the predicted

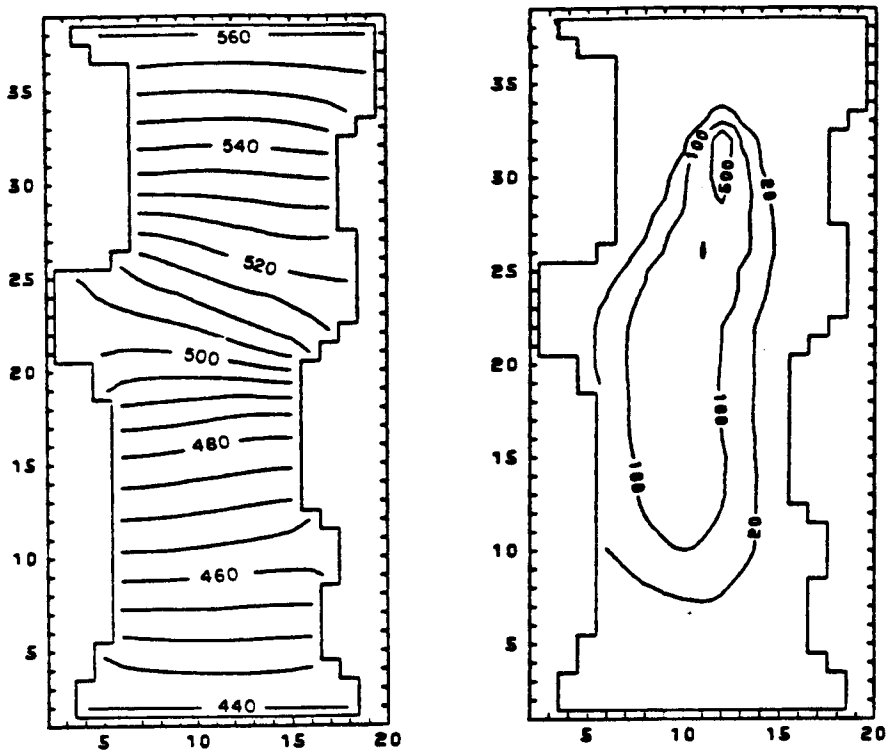

Figure 7-8. Predicted Hydraulic Head and Concentration Contours at the End of the Fifth Year, Using Parameters Determined with Data Strategy F (Interplolated Transmissivities) and Uncertainty Type I Data for PI-MOC Determined Dispersivities.

concentrations at the fifth year of simulation are shown in Figure 7-9. While spreading of the high concentration area appeared to be better than that in other cases, the transverse spreading of pollutants was too low. This was caused by the low estimates of transverse dispersivity (25 ft. to 29 ft.). It was interesting to note that the sum of squares analysis (Tables 7-4, 7-5, and 7-6) indicated that the concentration magnitudes were well preserved for large concentrations. However, the logarithm concentration sum of squares analysis (Tables 7-4, 7-5, and 7-6) showed that many smaller magnitude concentration estimates were significantly off due to the low transverse spreading of contaminant.

Among the other sampling strategies tested, strategies B and C were the best at giving parameters which preserved both plume shapes and concentration values. Results using sampling strategies A, B, C, and D, with six zone transmissivity parameterization and Type II uncertainty data are compared in Figure 7-10. From Figure 7-10, it can be seen that although adding more wells improved parameter estimates, it was not as effective as adding one year of data (compare strategies B and D to A). By comparing Figures 7-6 and 7-7, one can see that with increased observation over time, the predictions made by greater parameterizations improved. With sampling strategy A (Fig. 7-6), the improvement in concentration prediction at the fifth year of simulation with Type III uncertainty data is not as noticeable as it is with Strategy B (Fig. 7-7).

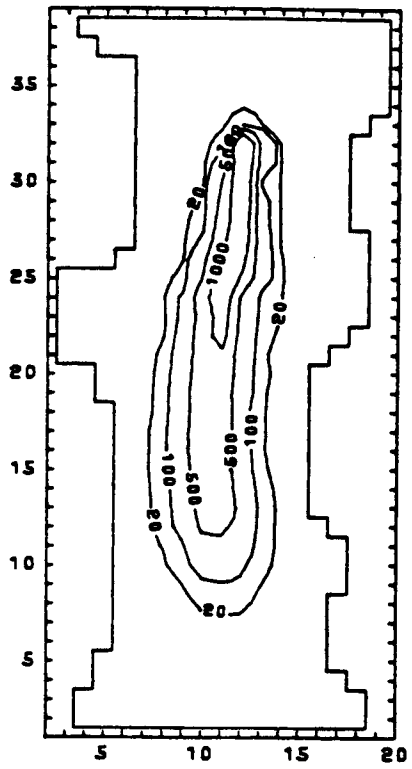

Figure 7-9. Predicted Concentration Contours at the End of the Fifth Year, Using PI-MOC Determined Parameters Found With Data Sampling Strategy E, Three Zone Transmissivity Characterization, and Data Uncertainty Type I.

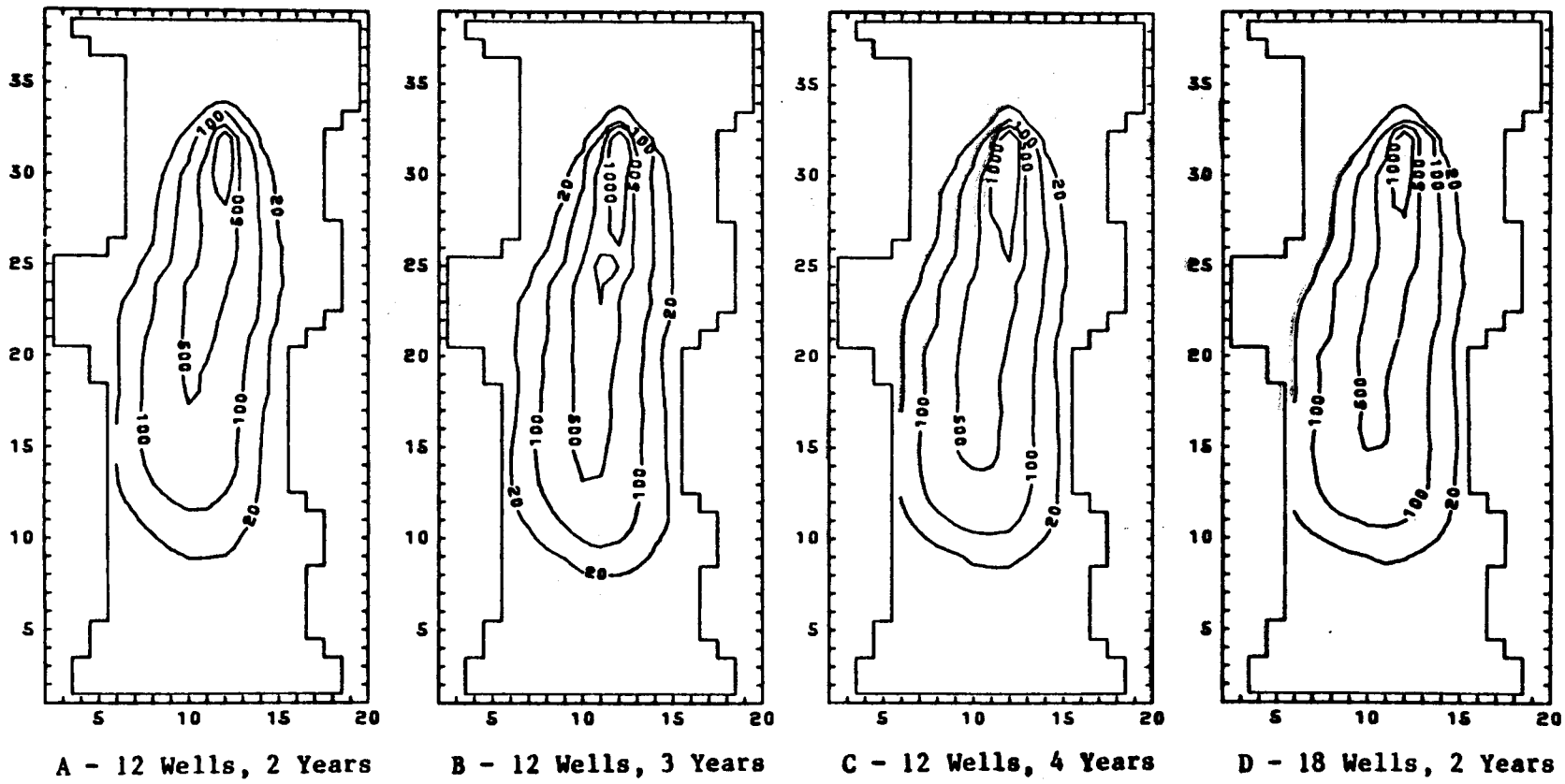

Figure 7-10. Comparison of Sampling Strategies A, B, C, and D. Concentration Predictions at the End of the Fifth Year, Using PI-MOC Determined Parameters from Type II Uncertainty Data, with Six Zone Characterization of Transmissivities.

Effects of Data Uncertainty

Increasing the uncertainty in the observations definitely made parameter estimation, and therefore predictions, worse. Data uncertainty also caused estimation difficulty for the PI-MOC algorithm. Particularly when the uncertainty level was high, PI-MOC could not find reasonable parameter estimates, unless the upper and lower bounds on transmissivity were manipulated. The choice of these bounds by the user had a significant effect on the parameter estimates. To show the effect of uncertainty on calibration, the actual plume shapes at the end of a five-year period are compared with those predicted from three zone parameterization (with all three uncertainty levels) in Figures 7-11 and 7-12. Generally, as uncertainty was increased, the improvement in prediction with more data (Strategy A versus Strategy B, for example) decreased with three zone transmissivity parameterization. By comparing the six zone parameterization of transmissivity for sampling strategies A and B in Figures 7-6 and 7-7, it can be seen that the additional year's worth of data significantly improved the prediction of concentration in five years. Given that a good characterization of the aquifer can be made, additional data taken over time can improve the concentration predictions significantly.

The PI method is formulated as an ordinary least squares approach which does not account for correlated residuals. To account for the correlated residuals, a generalized least squares approach would have to be used (Sadeghipour and Yeh, 1984). A generalized least squares approach, however, requires the estimates of serial correlation and the covariance matrix from the residuals. When data is limited, as in most practical applications and in

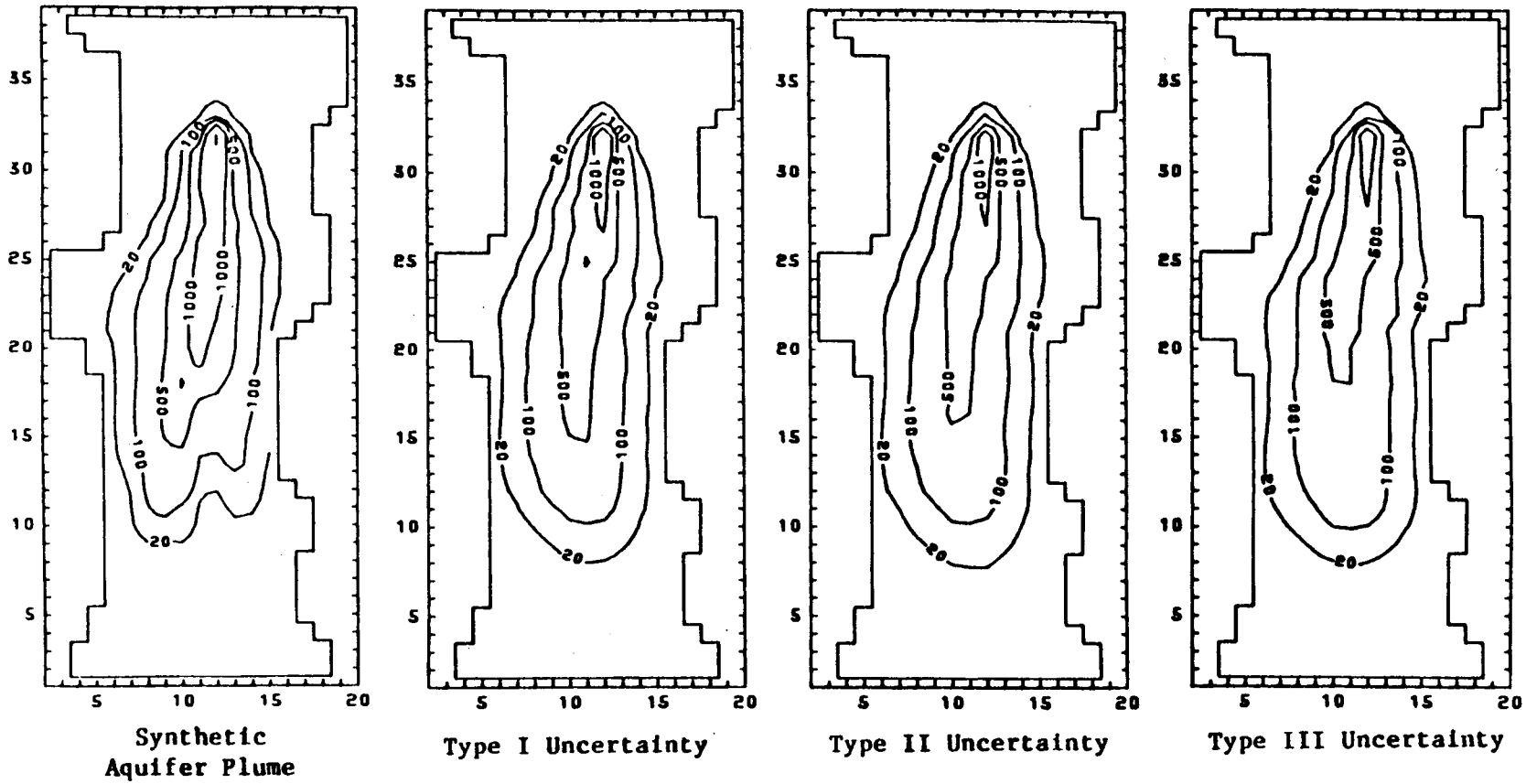

Figure 7-11. Comparison of Data Uncertainty Types on Concentration Predictions at the End of the Fifth Year, Using PI-MOC Determined Parameters from Sampling Strategy A (12 Wells, 2 Years), with Three Zone Transmissivity Characterization.

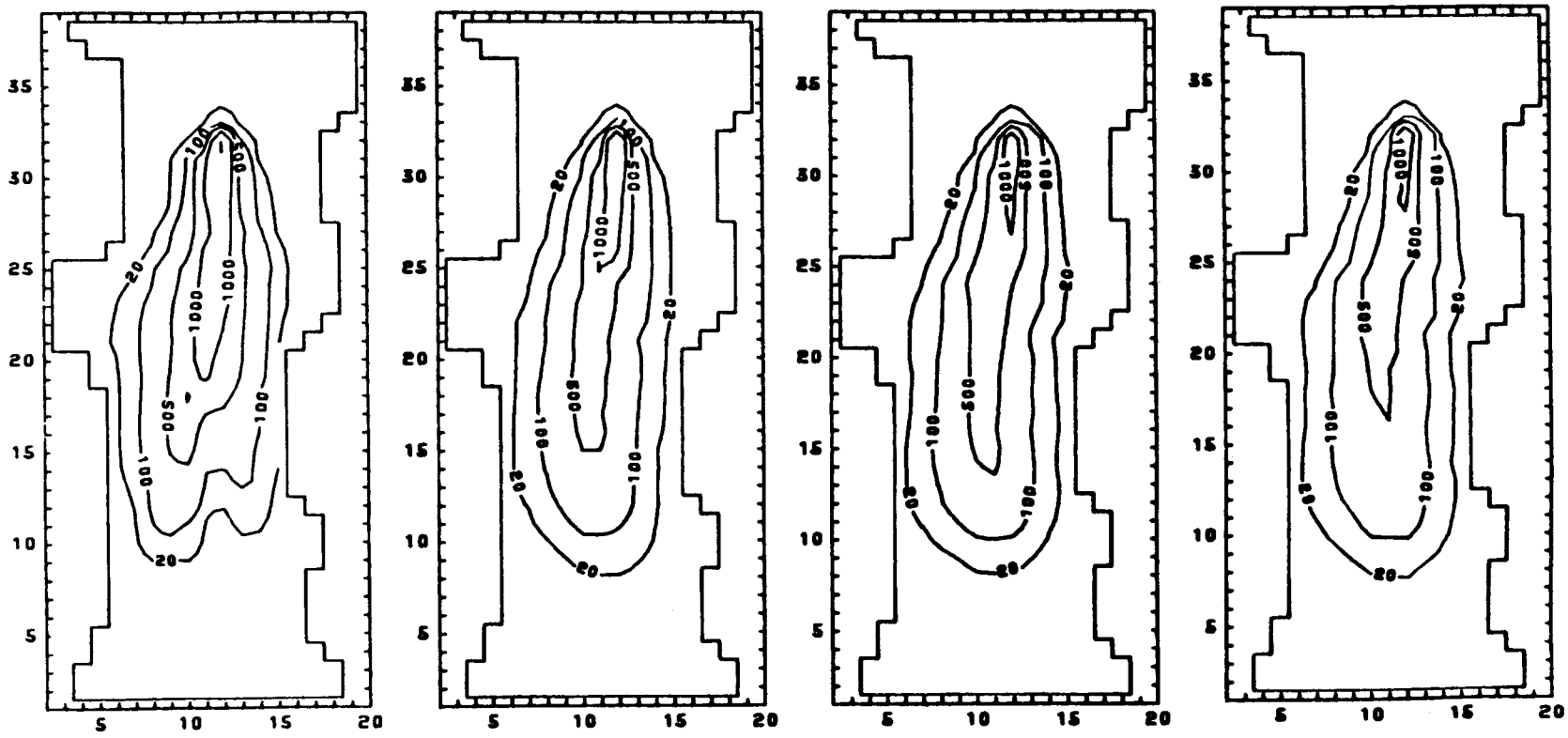

Figure 7-12. Comparison of Data Uncertainty Types on Concentration Predictions at the End of the Fifth Year, Using PI-MOC Determined Parameters from Sampling Strategy B (12 Wells, 3 Years), with Three Zone Transmissivity Characterization.

this study, the estimates of the covariance matrix are poor. Preliminary tests with the proposed PI-MOC code indicated that at least four years of monthly data (48 time steps) were required to get a reliable estimate of the covariance matrix. Serial correlation of the residuals could be estimated sufficiently well. Because of the limited data in all the cases examined (one of the objectives of this study was to investigate the effects of limited data), the generalized least squares approach to parameter identification was not used here, but would be recommended in cases where sufficient data was available.

CHAPTER 8

SUMMARY AND CONCLUSIONS

The data requirement issues in groundwater contaminant transport modeling have been examined in this study. A hypothetical, but realistic aquifer was created by an enlisted hydrogeologist. Using the synthetic aquifer data, the USGS-MOC model was used by the hydrogeologist to generate monthly hydraulic heads and concentration data for model calibration. The parameters and the responses of the hypothetical aquifer were kept unknown to the investigator until the end of the study. An automatic calibration (PI) algorithm was attached to the USGS-MOC model to aid in making the model calibration process more uniform and accurate. A special random field generator which preserves serial (lag one) and spatial correlations was created to represent uncertainties in the available observations. The noise generated by the random field generator was added to the generated monthly hydraulic heads and concentrations and became available for sampling. Three levels of uncertainty were investigated for their effects on parameter estimation. Different sampling strategies, which varied in the number of observation wells and length of record, were evaluated for their effects on parameter estimation. The effects of different parameterizations of aquifer parameters on model prediction were also investigated.

The major findings from this study can be summarized as follows:

1) The proposed PI-MOC algorithm can be used as an efficient tool for model calibration. The development of the algorithm was crucial for the evaluation of data requirements for this study. The results show that under

most of the realistic conditions examined, the algorithm was able to estimate aquifer parameters which enable the accurate prediction of the contaminant plume by USGS-MOC.

2) By using the estimated parameters from all the cases examined, each of the five-year predictions by USGS-MOC was able to preserve the general shape of the true hydraulic heads and contaminant plume contours. The accuracy in predicting the high concentration values (1000 units or more), however, varied from case to case. Most predictive runs underestimated high concentration values.

3) The most limiting sampling strategy (having eight observation wells with two years of monthly observations of hydraulic heads and concentrations) was identified as inadequate for accurate model prediction. The minimum data requirement for any reliable prediction in the synthetic aquifer was determined to be sampling strategy A (two years of monthly data in 12 observation wells).

4) Extending the time length of observations was more effective in improving parameter estimates than adding more observation wells. However, the incremental improvement from extending the time length of observation appeared to diminish over time.

5) It was found that, provided all boundary conditions are known, the accurate estimation of transmissivity in an aquifer was by far the most important step toward more reliable prediction of contaminant transport. The reason that parameters determined by PI-MOC only preserved the plume shape well (but not necessarily the actual concentration values) was due in a large part to the logarithmic transformation of the concentrations in the PI

objective function. However, further improvements to concentration estimates depend not on any transformation adjustment, but on a more refined estimation of transmissivity.

6) It was seen in this study that when calibration data were limited, significant errors in contaminant transport predictions resulted in only five years of simulations. We should be aware of the effects of limiting data on long term simulations of contaminant transport in future applications. We should also be aware that small errors in calibration results could be amplified in future simulation periods. Uncertainty analyses of the simulated results are imperative for future modeling applications.

7) It was found that the estimated transmissivity values from spatial interpolation produced results that were significantly inferior to those obtained from PI-MOC. It is felt that much improvement is to be gained by using the PI procedure if extended head and concentration observations are available. Additional pump test information will be very useful in delineating parameter zoning patterns, for providing prior estimates of model parameters, and for establishing upper and lower bounds on the parameters.

With the growing concern over our groundwater resources and the increasing popularity of groundwater models, it is suggested, based on the research results presented here, that extreme care be taken in using the predicted results from the models when only limited observations are available. It has been shown through carefully designed simulation experiments that the predicted results in a realistic application were significantly in error after only five years of simulation. Yet, in many

recent modeling studies, simulation results of 50 or even more than 1,000 years were used as a basis for planning or design practices. The development of digital simulation models offers an important and valuable avenue for solving groundwater problems. But, until we have obtained adequate and reliable data to properly calibrate these models, the use of their results for any design and planning practices should always be accompanied by thorough uncertainty analyses.

REFERENCES

Bachmat, Y., et al., 1980. Groundwater Management: The Use of Numerical Models, American Geophysical Union (AGU) Water Resources Monograph No. 5, AGU, Washington, D.C.

Bard, Y., 1974. Nonlinear Parameter Estimation, Academic Press, New York.

Buller, R.D., A. Gradet, and V.S. Reed, 1984. "Ground Water Monitoring System Design in a Complex Geologic Setting," Proc. of the Fourth National Symposium and Exposition on Aquifer Restoration and Ground Water Monitoring, National Water Well Association, Columbus, Ohio.

Cohen, R.M., and J.W. Mercer, 1984. "Evaluation of a Proposed Synthetic Cap and Concrete Cutoff Wall at Love Canal Using a Cross-Sectional Model," Proc. of the Fourth National Symposium and Exposition on Aquifer Restoration and Ground Water Monitoring, National Water Well Association, Columbus, Ohio.

Cooley, R.L., 1977. "Method of Estimating Parameters and Assessing Reliability for Models of Steady-State Groundwater Flow, 1, Theory and Numerical Properties", Water Resources Research, Vol. 13, No. 2, pp. 318-324.

Delhomme, H.P., 1979. "Spatial Variability and Uncertainty in Groundwater Flow Parameters: A Geostatistical Approach," Water Resources Research, Vol. 15, No. 2, pp. 269-280.

Frind, E.O., and G.F. Pinder, 1973. "Galerkin Solution of the Inverse Problem for Aquifer Transmissivity", Water Resources Research, Vol. 9, No. 5, pp. 1397-1410.

Gates, J.S., and C.C. Kisiel, 1974. "Worth of Additional Data to a Digital Computer Model of a Groundwater Basin," Water Resources Research, Vol. 10, No. 5, pp. 1031-1038.

Javandel, I., C. Doughty, and C.F. Tsang, 1984. Groundwater Transport: Handbook of Mathematical Models, Water Resources Monograph 10, American Geophysical Union, Washington, D.C.

Kitanidis, P.K., and E.G. Vomvoris, 1983. "A Geostatistical Approach to the Inverse Problem in Groundwater Modeling (Steady State) and One-Dimensional Simulations", Water Resources Research, Vol. 19, No. 3, pp. 677-690.

Konikow, L.F., and J.D. Bredehoeft, 1978. "Computer Model of Two-Dimensional Solute Transport and Dispersion in Ground Water", Chapter C2, Techniques of Water-Resources Investigations

of the United States Geological Survey, U.S. Geological Survey, Reston, Virginia.

Konikow, L.F., and D.B. Grove, 1977. Derivation of Equations Describing Solute Transport in Ground Water: U.S. Geol. Surv. Water-Resources Investigations 77-19, 30 pp.

Liggett, J.A., and P. L-F. Liu, 1982. The Boundary Integral Equation Method for Porous Media Flow, Allen and Unwin, Winchester, Massachusetts, 272 pp.

Matalis, N.C., 1967. Mathematical Assessment of Synthetic Hydrology, Water Resources Research, Vol. 5, No. 4, pp. 937-945.

Matern, B., 1960. Spatial Variation, Medd. Statens Skogsforskningsinst. Swed., Vol. 49, No. 5.

McLaughlin, D.B., 1984. "A Comparative Analysis of Groundwater Model Formulation: The San Andres - Glorieta Case Study", U.S. Army Corps of Engineers, Hydrologic Engineering Center, Davis, California, 75 pp.

Mejia, J.M., and I. Rodriguez-Iturbe, 1974. "On the Synthesis of Random Field Sampling From the Spectrum: An Application to the Generation of Hydrologic Spatial Processes", Water Resources Research, Vol. 10, No. 4, pp. 705-712.

Narasimhan, T.N., and P.A. Witherspoon, 1976. "An Integrated Finite Difference Method for Analyzing Fluid Flow in Porous Media", Water Resources Research, Vol. 12, No. 1, pp. 57-64.

Neuman, S.P., 1973. "Calibration of Distributed Parameter Groundwater Flow Models Viewed as a Multiple-Objective Decision Process Under Uncertainty", Water Resources Research, Vol. 9, No. 4, pp. 1006-1021.

Neuman, S.P., R.A. Feddes, and E. Bresler, 1974. Finite Element Simulation of Flow in Saturated-Unsaturated Soils Considering Water Uptake by Plants, Technion, Israel, Hydrodynamics and Hydraulic Engineering Lab., Report for Project No. ALO-SWC-77, 104 pp.

Pinder, G.F., and J.P. Bredehoeft, 1968. Application of the Digital Computer for Aquifer Evaluation, Water Resources Research, Vol. 4, No. 5, pp. 1069-1093.

Pinder, G.F., and W. Gray, 1977. Finite Element Simulation in Surface and Subsurface Hydrology, Academic Press, New York.

Prickett, T.A., T.G. Naymik, and C.G. Lonnquist, 1981. "A Random-Walk Solute Transport Model for Selected Groundwater Quality Equations", Bulletin No. 65, Illinois State Water Survey, Champaign Illinois.

Prickett, R.A., and C.G. Lonnquist, 1971. Selected Digital Computer Techniques for Ground Water Resource Evaluation. Bulletin No. 55, Illinois State Water Survey, Champaign Illinois.

Reddell, D.L., and D.K. Sunada, 1970. "Numerical Simulation of Dispersion in Groundwater Aquifers", Hydrology Paper No. 41, Colorado State University, Fort Collins, Colorado, 77 pp.

Remson, I., G. Hornberger, and F. Molz, 1971. Numerical Methods in Subsurface Hydrology, Interscience, New York.

Rodriguez-Iturbe, I., and J.M. Mejia, 1974. "The Design of Rainfall Networks in Time and Space", Water Resources Research, Vol. 10, No. 4., pp. 713-728.

Sadeghipour, J., and W.W-G. Yeh, 1984. "Parameter Identification of Groundwater Aquifer Models: A Generalized Least Squares Approach", Water Resources Research, Vol. 20, No. 7, pp. 971-979.

Salas, J.D., J.W. Delor, V. Yevjevich, and W.L. Lane, 1980. Applied Modeling of Hydrologic Time Series, Water Resources Publications, Littleton, Colorado. 404 pp.

Sampson, R.J., 1984. Surface II Graphics System, Kansas Geological Survey, Lawrence, Kansas, 240 pp.

Skaggs, R.L., 1984. "Model Study of Selected Mitigation Strategies to Control Radionuclide Migration in Ground Water", Proc. of the Fourth National Sympsosium and Exposition on Aquifer Restoration and Ground Water Monitoring, National Water Well Association, Columbus, Ohio.

Smith, L., and R.A. Freeze, 1979a. "Stochastic Analysis of Steady State Groundwater Flow in a Bounded Domain, 1, One-dimensional Simulations", Water Resources Research, Vol. 15, No. 3, pp. 521-528.

Smith, L., and R.A. Freeze, 1979b. "Stochastic Analysis of Steady State Groundwater Flow in a Bounded Domain, 2, Two-dimensional Simulations", Water Resources Research, Vol. 15, No. 6, pp. 1543-1559.

Sophocleous, M.A. 1984. "Groundwater-Flow Parameter Estimation and Quality Modeling of the Equus Beds Aquifer in Kansas, U.S.A.", Journal of Hydrology, Vol. 69, No. 2, pp. 197-222.

Trescott, P.C., G.F. Pinder, and S.P. Larson. 1976. "Finite-Difference Model for Aquifer Simulation in Two-Dimensions with Results of Numerical Experiments", Techniques of Water Resources Investigations of the U.S. Geol. Surv., Book 7, Chap. C1, 116 pp.

Umari, A., R. Willis, and P.L-F. Liu, 1979. "Identification of Aquifer Dispersivities in Two-Dimensional Transient Groundwater Contaminant Transport: An Optimization Approach", Water Resources Research, Vol. 15, No. 4, pp. 815-831.

Wang, C.P., and R.E. Williams, 1984. "Aquifer Testing, Mathematical Modeling,and Regulatory Risk", Ground Water, Vol. 22, No. 3, pp. 285-296.

Wang, J. and M. Anderson, 1982. Introduction to Groundwater Modeling - Finite Difference and Finite Element Methods, W.H. Freeman and Co., San Francisco, California.

Whittle, P., 1954. "On Stationary Processes in the Plane", Biometrica, Vol. 41, pp. 434-449.

Whittle, P., 1963. Stochastic Processes in Several Dimensions, Bulletin International Statistical Institute, Vol. 40, pp. 979-999.

Yakowitz, S., and L. Duckstein, 1980. "Instability in Aquifer Identification: Theory and Case Studies," Water Resources Research, Vol. 16, No. 6, pp. 1045-1064.

Yeh, W.W-G., 1975. "Aquifer Parameter Identification", J. of the Hydraulics Div., American Society of Civil Engineers, Vol. 101, No. HY9, pp. 1197-1209.

Yeh, W.W-G., 1985. "Review of Parameter Identification Procedures in Groundwater Hydrology: The Inverse Problem", Paper submitted to Water Resources Research.

Yeh, W.W-G., and Y.S. Yoon, 1976. A Systematic Optimization Procedure for the Identification of Inhomogeneous Aquifer Parameters, Advances in Groundwater Hydrology, Edited by A.Z. Saleem, American Water Resources Association, Minneapolis, Minnesota, pp. 77-82.

Yeh, W.W-G., and Y.S. Yoon, 1981. "Aquifer Parameter Identification with Optimum Dimension in Parameterization", Water Resources Research, Vol. 17, No. 3, pp. 664-672.